Post-Nourishment Beach Scarp Existence at the Sand Engine

MSc Candidate
John Darnall

June 2016

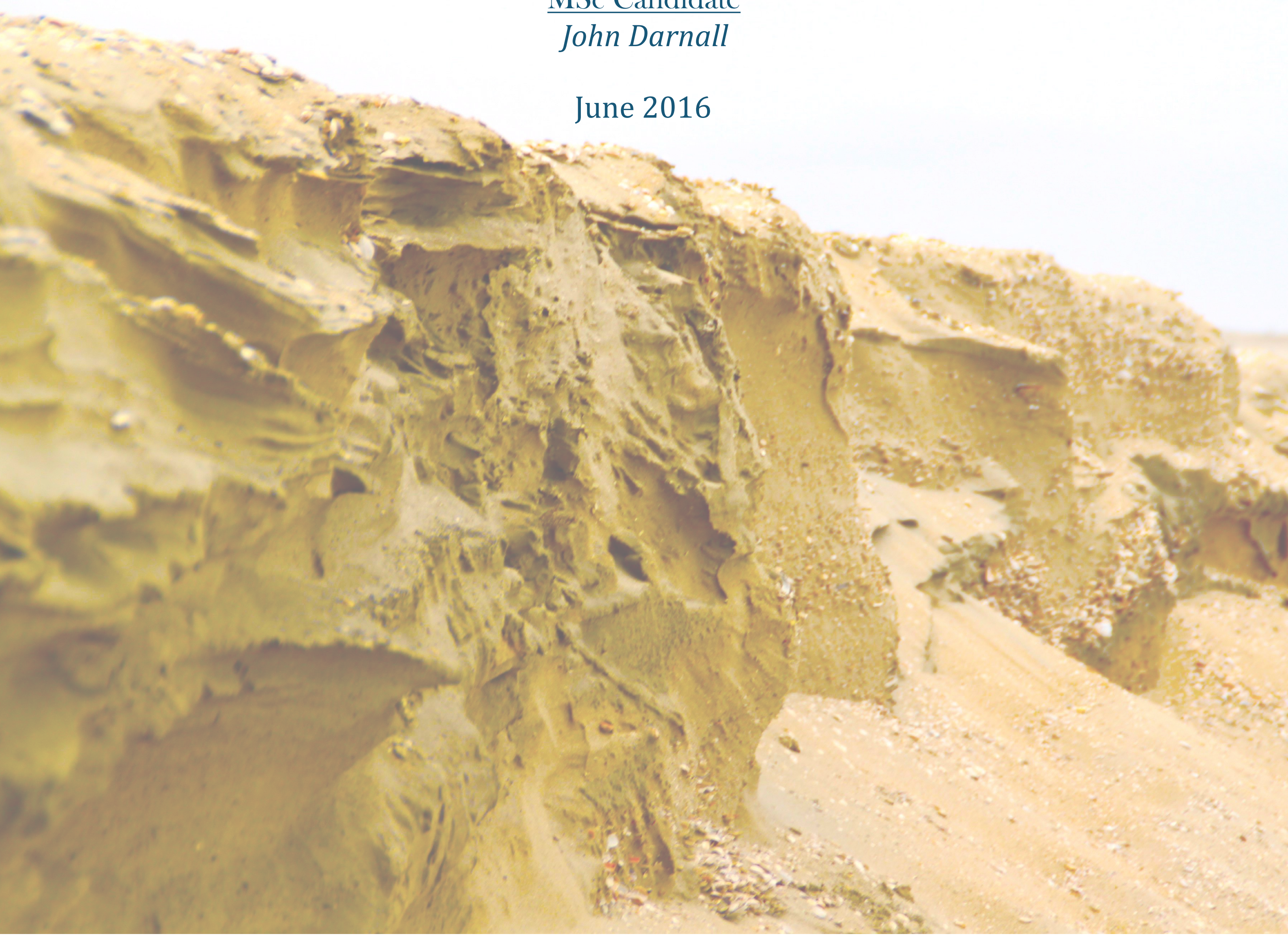

Erasmus Mundus MSc Program
Coastal and Marine Engineering and Management
CoMEM

Post-Nourishment Beach Scarp Existence at the Sand Engine

Delft University of Technology
June 27th, 2016

John Darnall
4434587

Post-Nourishment Beach Scarp Existence at the Sand Engine

MSc Candidate
John Darnall

Thesis Advisory Committee
Prof.dr.ir. A.J.H.M. Reniers (TU Delft)
Dr.ir. Matthieu de Schipper (TU Delft)
Dr.ir. Sierd de Vries (TU Delft)

Preface

Firstly, I would like to thank my Mom and Dad for their financial and moral support throughout this graduate program. This degree would not have been attainable without their unconditional love and generosity.

I would also like to give a very special thanks to my thesis advisory committee for their guidance and support throughout the research process; this committee includes Prof.dr.ir. A.J.H.M. Reniers, Dr.ir. Matthieu de Schipper, and Dr.ir. Sierd de Vries. Collaborating with you all has been an invaluable learning experience, and one that I will carry with me for the rest of my professional career. I look forward to potentially crossing paths again in the future, especially as the demand for coastal ingenuity in my home state of Louisiana increases. Also, thank you to Shore Monitoring & Management for allowing me access to the dataset making this study possible.

I would like to thank my CoMEM classmates for their support, generosity, and most importantly, friendship throughout the past two years. I feel extremely lucky in getting to share this experience with such an amazing group of individuals. There were 12 of us from 8 different countries and very diverse backgrounds, but we blended as a group from day one and took a sense of pride in each other's success. An old basketball coach of mine used to say "surround yourself with people who are smarter than yourself so your intelligence may never remain stagnant"; this could not be more true in that I was surrounded by all of your brilliant minds for two years and the knowledge I have gained is tremendous. I cannot thank you all enough for the good times and I look forward to working with you all at some point in the near future.

Finally, I would like to give a very special thanks to my classmate, roommate, and best-friend Gerald Songy. Not only did he introduce me to this program, but also would not accept 'no' for an answer. Turns out, you guided me into the single greatest experience of my life and I could not be more grateful for you and your friendship.

Abstract

A survey dataset taken at the Sand Engine mega-nourishment on the southwest coast of Holland was analyzed in an attempt to locate beach scarps and characterize their development. A beach scarp is defined as a vertical discontinuity in the upper foreshore slope generated through the removal of sediment by natural processes. More specifically, this report defines a scarp as a feature with a minimum height of 30 cm and a slope of 0.15. A few studies on beach scarp behavior have been investigated in recent years, but there is still quantitative ambiguity regarding the parameters that determine their post-nourishment generation, which can partially be attributed to their ephemeral nature. In turn, this lack of knowledge has directly hindered our ability to predict and/or prevent their existence in future nourishment projects.

Scarps were identified by use of an automated tool created to locate the steepest sections in the beach profile. This tool identifies the scarp crest (top) and toe (bottom) by the local minimum and maximum of the second order derivative of the profile elevations. Scarps were also identified by means of manual transect analysis to validate this automated process. These features were observed during 15 of the 33 measurement periods, with 8/15 being summer months and 3/15 being winter months. Thus, this scarping phenomena yields a strong seasonal signal with the majority of removal periods occurring during winter months when the wave climates were more energetic; however, it was also observed that calmer periods interrupted by storm events were also capable of altering scarp geometries. Scarping at the Sand Engine consistently occurred between +3 & +2 m NAP, with the average scarp height at the southern flank, head, and point being 0.85, 0.78 & 1.0 m respectively.

In general, scarps follow an overall pattern of periodic variability at the Sand Engine depending on the original profile geometry, water levels (storm surge & tidal elevation), and wave runup events. Observations showed that already developed scarps were only affected when the maximum runup levels (R_{HI}) exceeded the scarp toe (S_{LO}), which occurs during the collision, overtopping, and inundation regimes. The collision regime is responsible for the landward migration of the scarp without destroying the entire feature; the runup elevation is able to reach the scarp base inducing an undercutting effect which leads to slumping of the scarp face, but not necessarily to complete removal. Furthermore, scarps were completely removed only upon entering the overtopping and/or inundation regimes. It appeared the swash regime had no effect on the scarps at all considering the geometric characteristics remained approximately constant between measurement periods, insinuating the water levels were not high enough for the resulting runup to reach the scarp base. Thus, storm surge and tidal elevations have a strong influence on scarp generation/degradation at the Sand Engine, by exposing a greater area of the coast to wave attack.

Table of Contents

1. Introduction

1.1. Background

Coastal habitats and beaches are being threatened in many parts of the world due to increases in sea level rise and human intervention, along with decreases in sediment supply (Payo et al., 2008). The environmental, social, and economic implications of these circumstances are substantial considering almost half of the world's population lives or works within a couple hundred kilometers from coastal areas (Bosboom & Stive, 2015). Therefore, the need for studying/understanding coastal processes has exponentially increased in recent decades, in order to proactively mitigate erosional effects.

Sand nourishments have become an increasingly popular response to coastal erosion in many places around the world. These nourishments are used to increase beach width for recreational purposes and coastal safety (e.g. Dean, 2002; de Schipper et al. 2016). It is considered a "soft" measure in the field of coastal engineering as it enhances the local sediment budget while promoting a more sustainable mitigation technique. Although a more natural solution to coastal recession, it is not without its disadvantages. This mass input of sand causes large nearshore disturbances that equilibrate in time through sediment transport processes (Dean 1983; Elko et al. 2005; Ruiz de Algria-Arzaburu et al. 2013), and depending on the scale of the nourishment scheme, these disturbances can be quite significant.

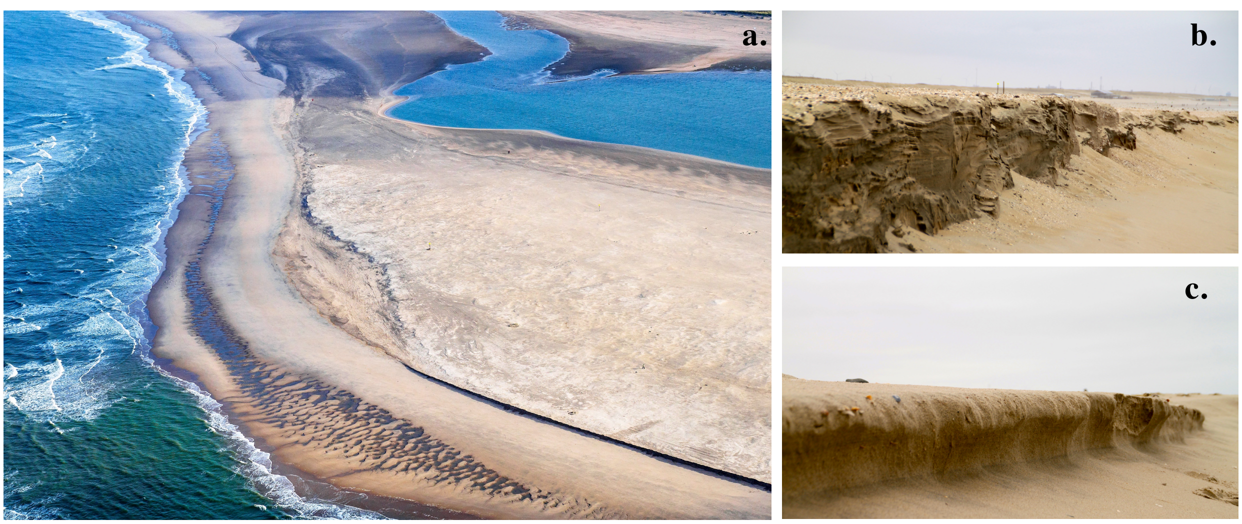

Figure 1.1 Beach scarping along the perimeter of the Sand Engine; (a) View looking Northeast on November 15th 2015. Image from the Dutch Ministry of Infrastructure and the Environment. (b) Beach scarp in the order of 90 cm. (c) Beach scarp in the order of 15 cm. Both images (b) & (c) were taken at the Sand Engine in February 2016.

Scarps are defined as ephemeral morphologic features with steep, nearly vertical, slopes (see figure 1.1). Beach and dune scarps are commonly observed following beach nourishment projects and/or high energy events. However, it is important to note that beach scarps and dune scarps are two different things; not only do they typically differ in orders of magnitude, but also in origin (Erikson et al. 2007). While much research has been conducted on understanding dune morphology in recent decades (e.g. Sallenger, 2000), beach scarp morphology remains a poorly understood subject (Ruiz de Algria-Arzaburu et al. 2013). Therefore, this report will focus on beach scarps, and one should assume beach scarping is meant if the type is left unspecified. A beach scarp is qualitatively defined by Sherman & Nordstrom (1985) as a vertical discontinuity in the foreshore slope generated by the removal of sediment from the lower beach by waves or currents. The two authors also state that scarp initiation indicates a change in the nearshore energy regime, inferring an alteration in wave or tidal characteristics. Furthermore, how this change in energy influences the moment of beach scarp generation is especially of interest because it will aid in future predictability.

This report will go on to describe the long- and cross-shore morphodynamics of beach scarps at the Sand Engine, and attempt to give semi-quantitative insight on the various parameters that influence scarp initiation and evolution.

1.2. Problem Description

Coastal morphodynamics according to Bosboom & Stive (2015) is the mutual adjustment of morphology and hydrodynamic processes involving sediment transport. In other words, changes in the morphology of a coastal system highly depend on the spatial and temporal fluctuations in transport rates within that system. The ability to predict coastal morphology on medium/large time scales (years to decades) based on hydrodynamics has significantly increased in recent years through experimental research and numerical modeling development. However, our ability to predict beach erosion and transport rates above the still water level on smaller time scales is still not ideal due to a lack of technology to accurately measure sediment concentrations and velocities in extremely shallow water, including the swash zone (Payo et al. 2008). Therefore, the hydrodynamics and resulting sediment transport in this region are not completely understood. Wright & Thom (1977) describe a nearshore morphodynamic system as one involving close coupling and feedback between process and form. This means that cause and effect are not easily observed on an immediate time scale due to the dynamic complexity of the system and its controls.

This research falls within the field of coastal morphodynamics where beach scarp initiation and evolution will be investigated at the Sand Engine mega nourishment in the Netherlands. It is very common to find scarps on sandy beaches after they are nourished as material is eroded near the waterline due to various hydrodynamic controls. This steep section in the foreshore profile can cause severe environmental, social, and economic implications (Kobayashi et al. 2009), and in some cases, retardation of post-storm recovery of the beach (Nishi et al. 1994).

A few studies on beach scarp behavior have been investigated in recent years (e.g. Bonte & Levoy, 2015; Ruiz de Algria-Arzaburu et al. 2013; Payo et al. 2008; Nishi et al. 1994; Sherman & Nordstrom, 1985), but there is still ambiguity regarding the physical parameters and quantitative characteristics which determine their development, which can be attributed to their ephemeral nature. In turn, this lack of knowledge has directly hindered our ability to predict and/or prevent their existence in future nourishment projects.

With beach nourishment projects becoming a more worldwide solution to coastal erosion, it is crucial to better understand this scarping phenomenon in order to maximize engineering efficiency.

1.3. Research Questions

The main research questions are as follows:

I. How do beach scarps develop in space and time along the perimeter of the Sand Engine?
   - Can beach scarps be identified utilizing the provided survey dataset?
   - If so, when and where do scarps exist in relation to the development of the cross-shore profile?
   - How do the following parameters correlate to beach scarp existence:
     - Foreshore slopes
     - Storm surge and tidal elevations
     - Wave forcing magnitude
   - Can the impact regime framework of Sallenger 2000 be applied to beach scarping at the Sand Engine?
   - Can beach scarp existence at the Sand Engine be predicted to some degree?

Ultimately, the main objective of this research is to give insight on post-nourishment beach scarp existence & development at the Sand Engine through bathymetric & hydrodynamic data analysis

1.4. Research Approach

To gain insight on post-nourishment scarp existence & generation at the Sand Engine, the specific research phases are as follows:

- **Phase 1**: Literature review of previous studies involving beach scarp morphodynamics
- **Phase 2**: Analyze Sand Engine survey dataset to identify and extract scarp-like features for all measurement periods
- **Phase 3**: Analyze the identified beach scarps and point out specific patterns in morphology
- **Phase 4**: Discuss delineations between form and process (morphology & hydrodynamics)
- **Phase 5**: Draw conclusions and give recommendations for future research

Figure 1.2. Flow diagram demonstrating the five phases of this MSc research project

1.5. Report Outline

Chapter 2 contains theoretical descriptions necessary for understanding the topics discussed in this research; followed by Chapter 3, which will introduce the study area and explain the details of the data analysis performed in the second research phase. Chapter 4 displays the results pertaining to the methodology and data analysis, which yields insight to spatial and temporal variations in beach scarping at the Sand Engine. Chapter 5 includes a detailed discussion of the aforementioned results displayed in Chapter 4, and offers mostly qualitative, but also semi-quantitative justifications for the patterns observed. Finally, Chapter 6 will summarize the findings of this research and give recommendations for future studies.

2. Theoretical Background

This chapter provides the necessary background for understanding the concepts and physical processes discussed in this report. The sections below describe these concepts in brief detail and one is referred to Bosboom & Stive (2015), Holthuijsen (2007), and Reniers & Roelvink (2012) for more detailed explanations, should another source be unspecified.

2.1. Coastal Zone

The coastal zone has been spatially defined in many different ways throughout the world. One reason there is no universal definition is due to the dynamic variability involved in these regions. In other words, coastline characteristics change quite drastically with geographical variation resulting in site specific definitions of the coastal zone. The spatial definition used in this report is after Sorensen (2006).

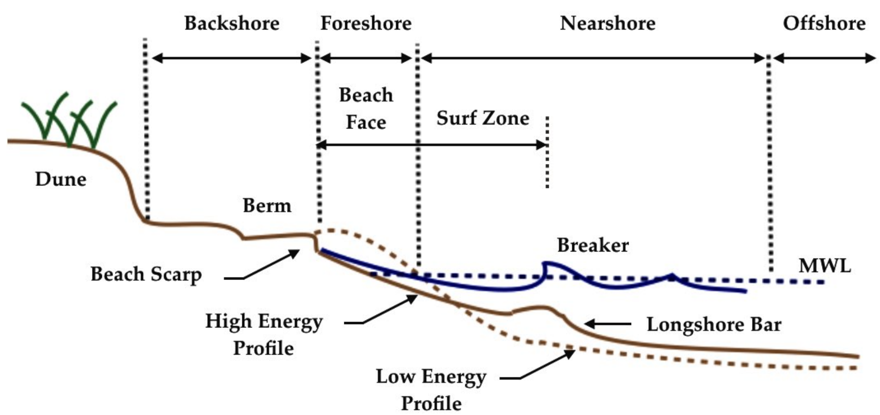

Figure 2.1. Spatial definition of the coastal zone after Sorensen (2006). This figure also demonstrates a beach scarp on the upper foreshore of the high energy profile.

It is important to note that the beach scarping phenomena discussed in this paper occurs on the upper foreshore section in the intertidal zone, which is the area of beach between low water and high water. Three dimensional features are commonly observed in this area due to variability in the nearshore energy regime and water levels.

2.2. Beach Nourishment

Beach nourishment, according to Bosboom & Stive (2015), is the addition of sand by artificial means in areas where sediment deprivation is causing problems. The main reasons for implementing a beach nourishment scheme are as follows: (1) to compensate for losses as a result of structural erosion, (2) to enhance the safety of the hinterland from flooding, (3) to widen a beach, create a new beach, or reclaim large areas of new land. The sediment added to the existing beach should be similar to the characteristics of the native material to avoid changing the morphological response too drastically. If the exact sediment size is not attainable, a slightly larger (coarser) size should be used to keep losses to a minimum.

In the case of structural erosion, strategic re-nourishment is a crucial aspect to the original design considerations in order to optimize the nourishment efficiency. This re-nourishment process is heavily dependent on the rate of erosion beyond the completion of the initial scheme. According to Bosboom & Stive (2015), five years is an acceptable amount of time between nourishments; however, it is important to note the uncertainty and associated risk that comes with these types of projects. For example, if a large storm occurs upon nourishment completion, the initial structural losses can be quite significant. Therefore, it is more logical to conduct beach nourishments of larger volumes in order to avoid continuous re-nourishment. Mega-scale nourishments, like the Sand Engine, are a newly applied concept with the intention of feeding adjacent coasts by means of alongshore diffusion (Stive et al., 2013). These large sand nourishments promote coastal sustainability in that they allow nature to do a large portion of the sediment reworking and deter frequent re-nourishment activities.

2.3. Beach States

Wright & Short (1984) distinguished a hierarchical classification system comprised of six different beach states. The two extreme states are referred to as dissipative and reflective, which are relatively two-dimensional and can be characterized by their cross-shore profile (Bosboom & Stive, 2015). In between these two extreme states are four intermediate cases which are far more three-dimensional. Each extreme state is described in more detail below:

- **reflective beaches** have steep cross-shore profiles with a relatively narrow beach face. They typically have berms on the upper shoreface, along with narrow surf zones without bars. Therefore, waves tend to break closer to shore if they break at all. If waves do not break, then the majority of the wave energy is reflected off the face of the beach. The Iribarren number associated with these beaches is larger than 2, which means the waves are generally of the surging or plunging breaker type.

- **dissipative beaches** consist of more mild slopes with a relatively wide surf zone consisting of bars. High energy waves tend to break further offshore due to the multiple linear bars and the shoaling effect of the wide surf zone. The Iribarren number (see section 2.5.2) associated with these beach profiles is fairly small (order of 0.2 - 0.3) meaning the beach itself is mostly subjected to spilling breakers; however, the surf zone is far more energetic due to high waves breaking further from the shoreline.

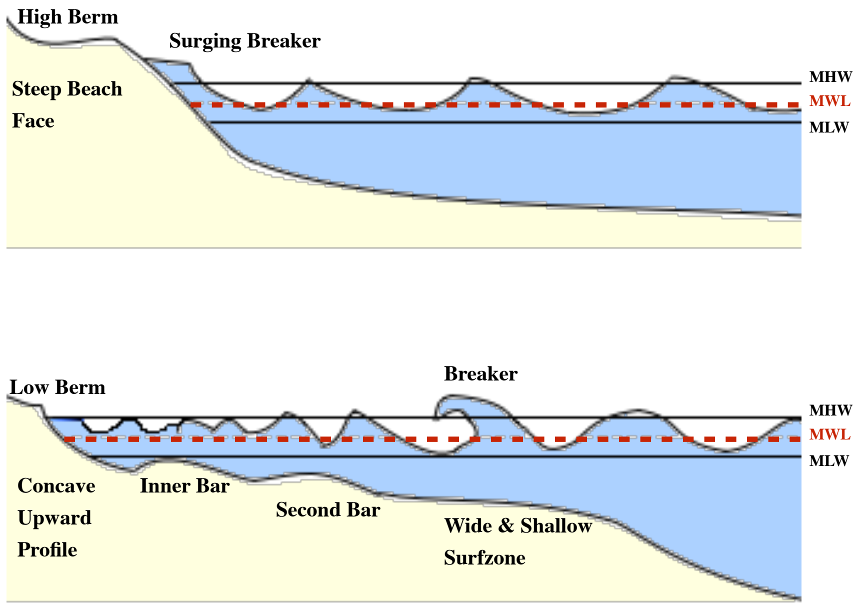

Figure 2.2 (Top) Reflective beach profile with a high berm and a less energetic surfzone. (Bottom) Dissipative beach profile with a low berm, wide & shallow surfzone, and sand bars. This figure was created after Wright et al. (1978). The red dotted line represents the mean water level in relation to mean high & low water levels.

The morphodynamic state of the surf zone and beach is extremely important to understand the nearshore morphology of any coastline. Nearshore ripples and bars can determine the locations and rates of energy dissipation due to wave breaking, which leads to insight on the morphological response of the beach (Wright and Short, 1984). Wright et al. (1985) found that future beach states were sensitive to past conditions; this effect is what is known as hysteresis, which means that present shoreline change is a function of past hydro- & morpho-dynamic conditions.

2.4. Wave Processes

2.4.1. Transformation

Waves undergo different transformations as they approach the nearshore region depending on the coastal setting under examination; this section will focus on wave shoaling, refraction, and breaking in particular. According to Bosboom & Stive (2015), wave transformation begins as the bottom depth reaches half the approaching wavelength.

- **Shoaling** is a process of energy concentration, which commences when the first wave in a wave train decreases in speed due to the fact that the wave begins to "feel" the bottom. The following waves, which travel at a faster speed, begin to catch up with the leading wave causing the wave height to increase.

- **Refraction** (see figure 2.3) is a transformation process which describes the bending of waves as they approach the nearshore. This change in direction of the wave crest is attributed to spatial variations in bottom depth. Assuming waves are traveling with a highly oblique angle of incidence, the part of the wave which reaches a shallower water depth first, decreases in propagation speed, allowing the opposite part of the wave (still traveling in deeper water) to catch up. This process explains why waves tend to align their crest perpendicular to the shore normal.

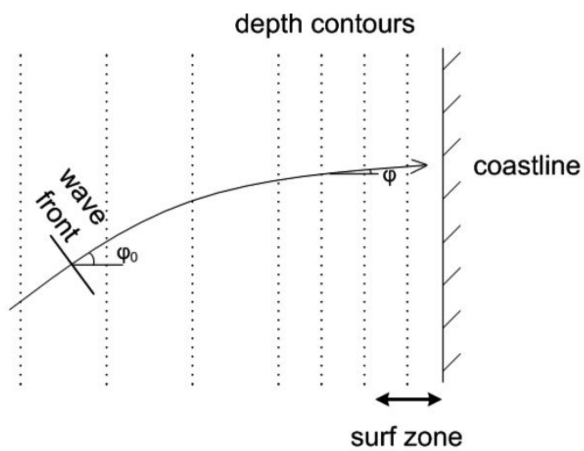

Figure 2.3 Obliquely incident waves traveling from from deep water over uniform depth contours taken from Bosboom & Stive (2015).

Snell's law makes use of both the angle of wave approach and wave celerity at location 2 different locations to describe this effect:

$$\frac{\sin\phi_o}{c_o} = \frac{\sin\phi}{c} \qquad (2.1)$$

where (ϕ_0) and (ϕ) are the angles of wave approach taken at locations in deep and shallow water respectively; (c_0) and (c) represent the wave celerities corresponding to those same locations in deep and shallow water. The wave celerity [$c = L/T$]. can be calculated by dividing the corresponding wave length (L) by the wave period (T), and represents the velocity of the wave crest.

- **Wave Breaking** is the process in which waves dissipate their energy in the nearshore region referred to as the surfzone. The shoaling process leads to a continuing increase in wave height until the crest becomes unstable due to increasing particle velocities at the crest. Once the wave steepness becomes too large, the wave breaks causing alongshore currents in the breaker zone. It is important to note that wave breaking can also occur in deeper water where it is dependent on wind velocities, rather than water depth.

2.4.2. Runup

Wave forces can have a significant effect on the overall morphology of any coastline, considering they induce both mean water level fluctuations (setup and setdown) and long- and cross-shore currents (Bosboom & Stive, 2015). One result of wave forcing in the intertidal is referred to as wave runup (R) , and can be defined as the landward extent of wave uprush measured vertically from the still water level; it consists of wave setup and swash according to Melby et al. (2012). Swash is the water that washes onto the intertidal platform as a result of wave breaking. Holman (1986) found the 2% exceedance of run-up ($R_{2\%}$) & swash ($S_{2\%}$) as follows:

$$R_{2\%} = H_0\,[0.83\,\xi + 0.2] \qquad \text{……………………..} \qquad (2.2)$$

$$S_{2\%} = H_0\,[0.85\,\xi + 0.06] \qquad \text{……………………..} \qquad (2.3)$$

where H_0 is the offshore wave height, and ξ is the Iribarren parameter. Battjes (1974) classified wave breaking according to the Iribarren parameter (Iribarren and Nogales 1949):

$$\xi = \tan\alpha/(H_0/L_0) \qquad \text{……………….……} \qquad (2.4)$$

where α is the local foreshore slope and L_0 is the offshore wave length; (1) spilling breakers correspond to [$\xi < 0.5$], (2) plunging breakers correspond to [$0.5 < \xi < 3.3$], (3) surging & collapsing breakers correspond to [$\xi > 3.3$].

Sallenger (2000) defines representative high and low runup elevations in order to create a framework for barrier island impact assessment; his formulations are as follows:

$$R_{HIGH} = R_{2\%} + \eta_{avg} \qquad \text{……………….……} \qquad (2.5)$$

$$R_{LOW} = R_{HIGH} - S_{2\%} \qquad \text{……………….……} \qquad (2.6)$$

where (η_{avg}) is considered to be the mean water level, which increases during extreme storm events due to a phenomenon referred to as storm surge. During an extreme storm event, waves generated in the open sea are much higher than that of moderate conditions; according to (Bosboom & Stive, 2015), water piles up at the coastline raising the still water level for the duration of the storm due to extreme winds. This event can potentially make higher elevations in the profile susceptible to wave attack.

These runup formulas and parameters will be referenced again in Chapter 4 of this report, where a reference framework for beach scarp regime changes will be discussed and validated with a survey dataset from the Sand Engine.

2.5. Sediment Transport

Sediment transport is the link between the waves and currents and the morphological evolution of the coast (Reniers & Roelvink, 2012). The two authors also state that sediment transport is a strong and non-linear function of current velocity and orbital motion, sediment properties, and the bed roughness. It can be divided into different categories based on the relative location in the water column (bed- and suspended-load transport) and the direction of movement in relation to the shoreline (long- and cross-shore transport).

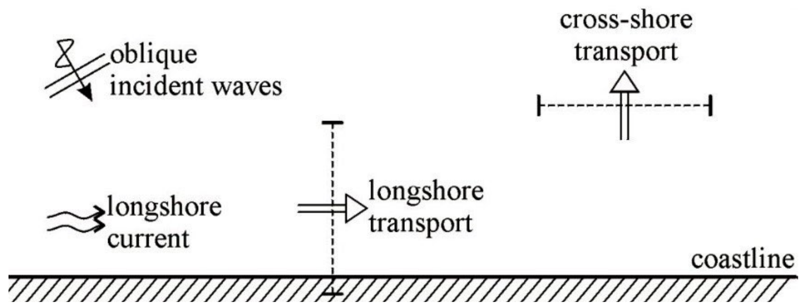

Figure 2.4. Schematic representation of cross-shore and longshore transport orientations Taken from Bosboom & Stive (2015)

Cross-Shore Transport

Cross-shore transport is mainly wave driven and is defined by different mechanisms which can either be on- or off-shore directed; such mechanisms are briefly described below and include undertow, Longuet-Higgins streaming, Stokes' drift, and long-short wave interaction.

- **Undertow:** is the offshore directed current in the surf zone below the wave trough level resulting from compensating the onshore directed flow; the undertow mass transport is larger under breaking waves. According to Bosboom & Stive (2015), there should be a zero net mass transport through the vertical in the presence of a closed boundary (i.e. coastline) due to continuity, which induces this return current.

- **Streaming:** is an onshore directed, non-zero wave-averaged flow near the bed due to wave energy dissipation in the boundary layer caused by friction. This becomes a less important phenomena in the surf zone due to the wave breaking and undertow.

- **Long-short wave interaction:** produces a net off-shore sediment transport when the correlation between the short waves and the long wave is negative; this relationship may change due to the release of the bound long waves, as a result of the breaking of short waves.

Longshore Transport

Coastline change is a result of gradients in transport rates, and may occur due to changes in nearshore wave height and angle of wave incidence leading to erosion or deposition. Longshore sediment transport is the net movement of particles parallel to the shoreline. According to Bosboom & Stive (2015), coastline change is dominated by alongshore effects in the case of human induced changes (e.g. beach nourishments). Wave driven longshore sediment transport depends heavily on the hydrodynamics in the breaker zone and sediment characteristics.

Longshore current velocities are predominantly driven by the tide and breaking waves approaching at an oblique angle of incidence; this current is generally concentrated in the surf zone. The breaking wave forces act to stir up sediment on the beach and the resulting current velocities transport sediment to adjacent sections of the beach. Therefore, in theory, the larger the nearshore energy due to wave breaking, the larger the gross sediment transport.

2.6. Chronology of Studies Related to Beach Scarps

The definition of a beach scarp according to Sherman & Nordstrom (1985) is a vertical discontinuity in the foreshore slope induced by an increase in the nearshore energy regime. They are most commonly observed on steeper beaches following a nourishment project and/or extreme storm event; however, extreme events may also lead to the destruction of scarps as well, partially due to increasing water levels (e.g. Payo et al., 2008). Not only are these morphological features commonly observed on newly nourished beaches, but also on many natural beaches around the world (Sherman & Nordstrom, 1985; Carter, 1988; Short, 1999; Vousdoukas, 2012). Furthermore, Sherman & Nordstrom (1985) separate beach scarps into two classifications based on the mechanism of initiation. The first classification is referred to as process controls; this includes hydrodynamic processes acting in the along- and cross-shore directions, such as swash motions. The second classification is referred to as structural controls; this includes vertical and horizontal controls, such as beach freezing and lee effects of protective coastal structures. The two authors also concluded beach scarping was independent of large-scale geographical controls, such as latitude and longitude, based on occurrences in contradicting climates (e.g. Mediterranean coast versus California coast; the latter being more energetic).

Nishi et al. (1994) conducted field observations on the Pacific Coast and East China Sea Coast in an attempt to study geomorphological characteristics of dune and beach scarps, followed by a numerical study to analyze scarp generation using the SBEACH model. In particular, they found the foreshore slope to be of importance to scarp initiation. Therefore, they applied regular waves (H = 2.3m; T = 6s) to a beach with uniform slopes of 1/10, 1/15, and 1/20. It was found that the steeper the initial beach profile, the larger was the resulting scarp. They also discovered the smallest beach width corresponded to the largest scarp height (and visa versa), due to increased erosion of the scarp face and upward migration into the profile. The authors hypothesize developed scarps to slow down post storm recovery by less energetic waves due to reflection off the scarp face. A longshore curved scarp distribution was recorded during one of their observations, insinuating that longshore sediment transport played some role in beach scarp generation. Nishi et al. (1994) attributed this curved distribution to an incident wave field of uneven heights, most likely caused by an offshore island or borrow pit. Payo et al. (2008) also noted alongshore variability in their experimental results, but said it was most likely due to a non-uniform slope in a supposedly uniform wave basin. Seymour et al. (2005) noted that scarping resulted in alongshore quasi-periodic variability, but the causes were unidentified.

Payo et al. (2008) proposed a simple procedure to improve predictive capability for scarping erosion above the still water level , by conducting an experiment in a multi-directional wave basin. The authors build upon the sediment transport model of Schmied et al. (2006) through the additional considerations of bottom slope and scarping effects. Two experiments were conducted by applying normally incident, irregular waves to different berm geometries (horizontal berm and tilted berm). The model performance was then graded using the Brier Skill Score (BSS), for which it gave good predictability of profile changes above the still water level for the horizontal berm test; however, fair predictability was found for the tilted berm test, but the authors attribute this to a ponding mechanism as the water levels were increased. It is also important to note the most accurate results were given when the roller effect and bottom slope of the foreshore were included in the analysis.

Ruiz de Algria-Arzaburu et al. (2013) studied the morphological evolution of beach scarps of large dimensions on a nourished Caribbean beach. The authors evaluated surveys every three to four months over the course of 1.5 years, and identified scarp tops (crests) and bottoms (toes) from the minimum and maximum second order derivatives of the profile examined. Furthermore, features were only deemed scarps if the slope was larger than the critical angle of repose (32^{o}) and the height was larger than 0.25 m. It was concluded that runup, tidal elevation, and longshore energy flux accounts for 40% of the cross-shore morphological evolution of beach scarps. According to Larson et al. (1999) and Jackson et al. (2010), the persistency of beach scarps heavily depends on wave overtopping and water levels during storm events, and the local beach conditions (Bonte & Levoy, 2015).

Bonte & Levoy, (2015) conducted a field experiment by creating an artificial beach scarp along a macro-tidal beach during oblique wind-wave conditions. They investigated the relationship between wave impacts induced by swash, water level, and beach scarp retreat trajectory. Swash activity and topographic characteristics were measured using video imaging and a terrestrial laser scanner, respectively, in order to develop a new dataset for assessment. Image time stacks were used to analyze swash motions on the face of the scarp over one tidal cycle, where a strong connection was identified between local beach evolution and scarp alterations. In other words, the foreshore elevation and slope caused by longshore sediment transport due to obliquely incident waves was believed to have some effect on the swash activity. Within this context, they found as the local beach level was lowered, scarp erosion increased (and visa versa), which reinforces the importance of water level and foreshore slope during energetic events. In accordance with Nishi et al. 1994, the authors also discuss the influence beach scarps have on swash motions. It is believed reflection of the wave uprush on the scarp face causes a collision between the reflected backwash and the subsequent uprush. These collisions can reduce the motion of the following uprush event which allows the scarp face to avoid swash impact, and ultimately leads to natural scarp preservation.

While many studies have been conducted in recent years on the morphology and physical processes affecting *dune* scarps, quantitative information on *beach* scarp formation and evolution is still not well defined (Bonte & Levoy, 2015) . This is attributed to a lack of sufficient field datasets and limited measuring capabilities in the intertidal zone (Payo et al. 2008), especially during storm events. Thus, most reliable datasets consist of pre/post-storm surveys in order to assess the profile changes over that specific time period.

2.7. Lifecycle & Impact Scale

Based on the important parameters discovered from the literature review discussed in the previous section, a first-order framework was created describing the lifecycle of a typical beach scarp. This section will go on to explain what this estimated life-cycle entails, and will display a schematization of the hypothesized regime changes; this regime change concept was taken from Sallenger (2000) and altered to fit within the context of this report. Sallenger (2000) created a storm impact scale for the dunes of barrier islands to demonstrate the varying parameter thresholds. In this report, his framework was translated to the upper foreshore and applied to beach scarps. The terminology of the scarp characteristics in relation to the run-up is displayed in figure 2.5, where S_{HI} & S_{LO} represent the scarp crest (top) and toe (base) elevations respectively. R_{HI} and R_{LO} are taken as representative high and low swash elevations relative to a fixed vertical datum (Sallenger, 2000); parameters include water elevations due to storm surge, astronomical tide, and wave run-up. Figure 2.5 will be referred to throughout this section of the report.

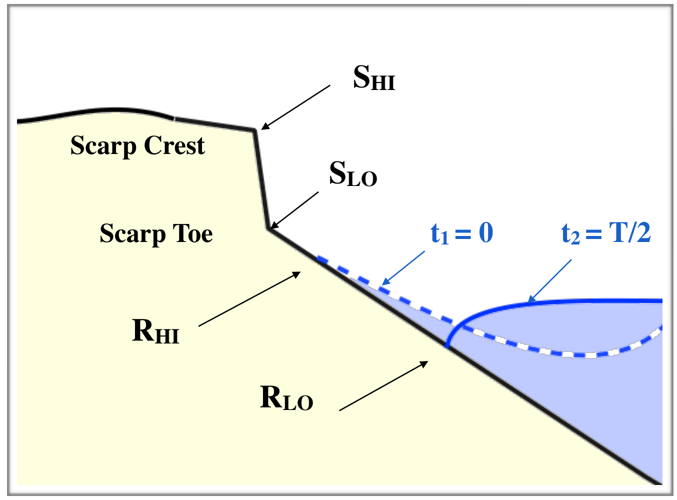

Figure 2.5 Beach scarp schematic and terminology (After Sallenger, 2000) demonstrating the scarp crest (S_{HI}) and scarp toe (S_{LO}) in relation to the runup (R_{HI}) and rundown (R_{LO}) levels.

2.7.1. General Profile Development

For the most part, beach scarp evolution is vaguely understood in a qualitative sense. In light of this, the post-development behavior of beach scarps has been explored in more detail in recent years. However, quantitative information describing the physics responsible for beach scarp initiation is still heavily lacking. Instantaneous measurements would be required to yield insight on the physics of this initiation process, which was beyond the scope of this report. Sherman & Nordstrom (1985) qualitatively describe the controls they believe to be partly responsible for beach scarp initiation and separate them into two categories: process controls and structural controls. Process controls are things such as wave run-up, swash, and tidal currents; whereas structural controls are characteristics of the beach itself (e.g. beach slope & sediment temperature).

Sherman & Nordstrom (1985) go on to give an example of ideal scarping conditions which included an equilibrium profile with a high berm and a steep foreshore slope. An increase in wave energy and wave steepness during high energy events will cause the lower foreshore slope to decrease due to sediment mobilization; while the upper foreshore slope increases due to deposition caused by large swash infiltration rates above the beach water-table.

Once the slope becomes steep enough, the swash motions will continually impact the face of this newly developed feature. Generally, the swash motions attack the toe of the scarp inducing an undercutting effect; this causes instabilities in slope which may lead to slumping or liquefaction. Slumping is best described as a shear failure of a 'slice' of the foreshore, which often results in a beach scarp. Liquefaction occurs when the critical pore water pressure of sediment being impacted in the foreshore is surpassed; a shallow failure is the typical result, which can also aid in steepening the profile. The slumped volume of sediment will temporarily protect the toe of the scarp until it is removed through repeated swash motions; at which time, the undercutting process recommences.

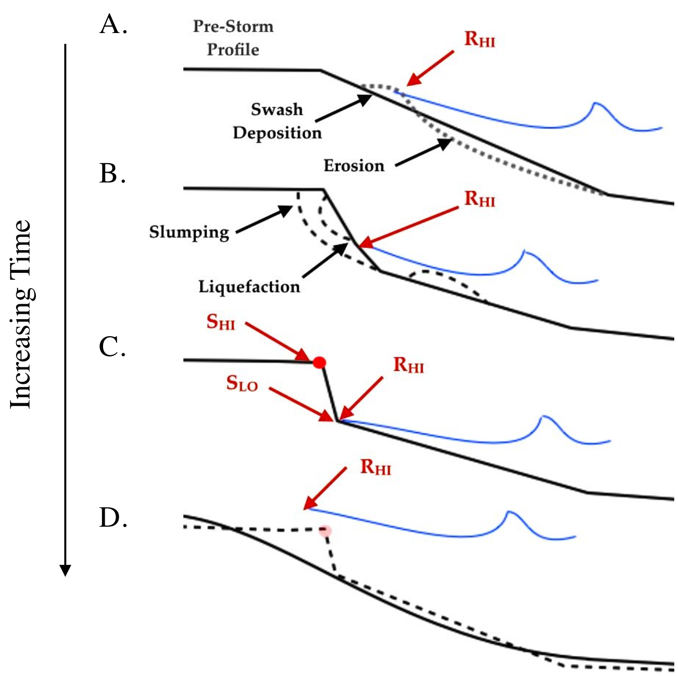

Figure 2.6 Hypothesized schematization of the life cycle of a beach scarp. (A) The dotted line represents the early erosional response of the profile to a high energy event. (B) The lower foreshore continues to develop a more concave profile with respect to the incoming waves, steepening the slope of the newly developed berm; as the water collides with the base of the scarp, the toe will begin to erode inducing a slumping or liquefaction failure. (C) The profile has been undercut through swash motions and the profile has steepened into a newly developed scarp, with the red dot indicating the scarp crest (S_{HI}). (D) R_{HI} surpasses S_{HI}, leading to the removal of existing scarps.

This process will continue on until the water levels and wave overtopping events become too large for the scarp to sustain; thus, majority of scarps are destroyed when (R_{HI}) becomes larger than the scarp crest (S_{HI}). However, should the hydrodynamics fail to destroy the scarp within the high energy duration, they will remain until the water levels and wave energy become large enough to induce change. Also, as the sand dries, aeolian transport processes may lead to the subtle demise of scarps as a result of high wind speeds; however, the latter is something that would occur over a longer time period.

2.7.2. Regime Changes

The previous section provided a general overview of the hypothesized lifecycle of a beach scarp from its ambiguous initiation, to its ultimate demise; however, this section will explain the regime changes which take place as a result of runup events in a step-by-step manner, and will yield insight on the various parameter changes throughout the evolution process. This paper makes use of the impact regime framework of Sallenger (2000), in an effort to characterize the development of beach scarps in the upper foreshore. It is important to note that this section assumes a scarp is already in existence (Profile C in figure 2.6) and the highest water levels are in effect.

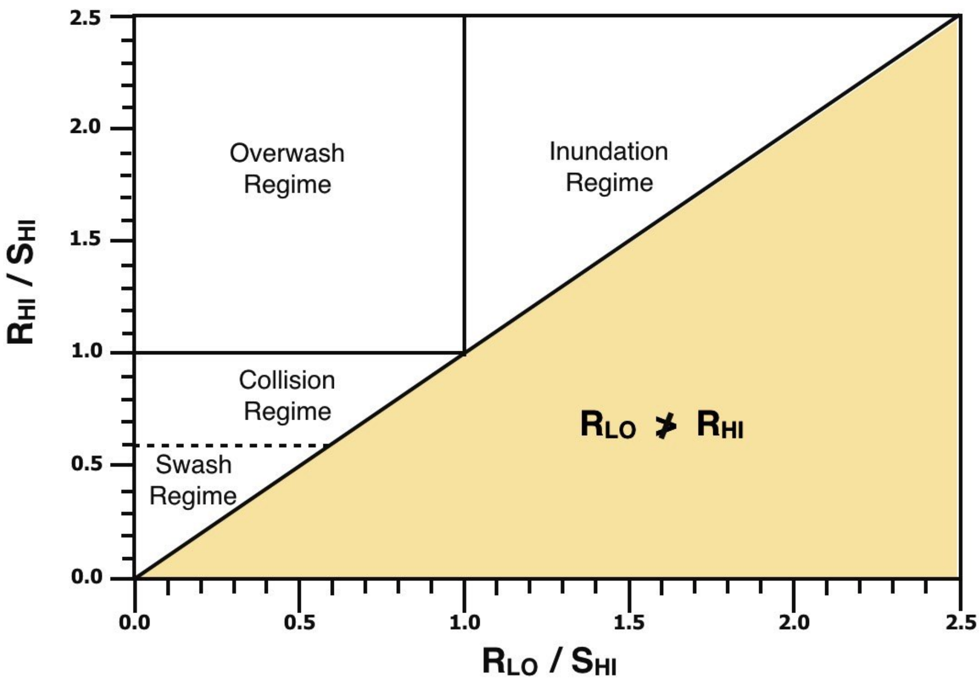

Figure 2.7 Schematic of impact regime changes after Sallenger (2000). (I) The 'swash' regime occurs when $R_{HI} / S_{HI} << 1$. The runup levels are confined to the lower foreshore section of the existing beach and therefore are not high enough to influence the beach scarp too drastically. (II) The 'collision' regime occurs when the runup becomes large enough to reach the base of the scarp; typically, the toe will be eroded away as the scarp is impacted by the swash motions. (III) The 'overtopping' regime begins once $R_{HI} / S_{HI} = 1$; the runup levels exceed the scarp crest. (IV) The 'inundation' regime occurs when $R_{LO} / S_{HI} = 1$; R_{LO} surpasses the scarp crest elevation and the upper part of the profile is completely subaqueous.

"Swash Regime"

The swash regime occurs when the wave run-up is confined to the lower foreshore section of the existing beach. Therefore, the water levels are not large enough for the resulting run-up to influence the beach scarp too drastically. R_{HI} may reach the scarp toe during this regime, depending on the wave energy. Should the R_{HI} reach S_{LO}, this regime may lead to small changes in the scarp geometry; however, if R_{HI} does not reach S_{LO}, the scarp is thought to be unaffected. Therefore, the swash regime occurs when R_{HI} / S_{HI} is less than the critical threshold defined in equation 2.7 below.

$$R_{HI} / S_{HI} = S_{LO} / S_{HI} \qquad \text{2.7}$$

"Collision Regime"

The collision regime occurs when the critical threshold defined in equation 2.7 is exceeded. R_{HI} becomes large enough to reach the base of the scarp on a consistent basis, collapsing the scarp face. Typically, the base will be eroded away as the scarp is impacted by the uprising swash, which will cause slope instabilities in the higher part of the profile; this generally leads to slumping (see figure 2.6). The scarp will continue to migrate upwards into the profile as a result of repetitive slumping until the maximum slope is reached, or the water levels increase. Similar to the swash regime, the collision regime will also result in erosion of the lower foreshore, especially as water levels lower and storm surge subsides.

Nishi et al. (1994) hypothesize developed scarps to slow down post-storm recovery by less energetic waves due to reflection off the scarp face, which would fall within this regime. The authors believe reflection of the wave uprush on the scarp face causes a collision between the reflected backwash and the subsequent uprush. Furthermore, the authors suggest these interactions may reduce the motion of the following uprush event, which allows the scarp face to avoid impact and ultimately leads to natural scarp preservation.

"Overtopping Regime"

The overtopping regime commences once R_{HI} exceeds the scarp crest. Generally, R_{LO} is slightly larger than or equal to the scarp toe elevation allowing the scarp crest to be overtopped by the incoming uprush of energetic waves. If the overtopping events are persistent enough, this can lead to smoothing of the slope, or the destruction of the scarp. However, should the scarp not be destroyed due to overtopping events, this regime may lead to longshore variabilities in scarp geometry and a net landward movement of the upper beach edge. As the resulting runup overtops the scarp crest, water is allowed to flow landward which may lead to deposition in the upper profile.

$$R_{HI} / S_{HI} = 1 \qquad \text{2.8}$$

"Inundation Regime"

The inundation regime occurs when R_{LO} reaches the scarp crest elevation. In this scenario, the upper part of the profile is completely subaqueous and basically acts as the traditional surf zone. This regime generally leads to the demise of beach scarps on the upper foreshore and also to a net transport of sediment in the onshore direction due to the overwashing waves. This regime is typical of extreme events such as hurricanes and tropical storms.

$$R_{LO} / S_{HI} = 1 \qquad (2.9)$$

3. Methodology

3.1. Study Area

The Sand Engine is a mega-nourishment positioned along the southwestern region of the Dutch coast between the harbour entrances of Scheveningen and Hoek van Holland (see figure 3.1.B.). The project, which entailed the addition of 21.5 million cubic meters of sand, was completed in July of 2011. Prior to its construction, this 17 km stretch of coast (Westland coastal cell) on the North Sea experienced a shoreward recession of nearly 1 km between 1600-1990 (de Schipper et al., 2016), despite various mitigation strategies including rubble mound groins and smaller nourishment schemes.

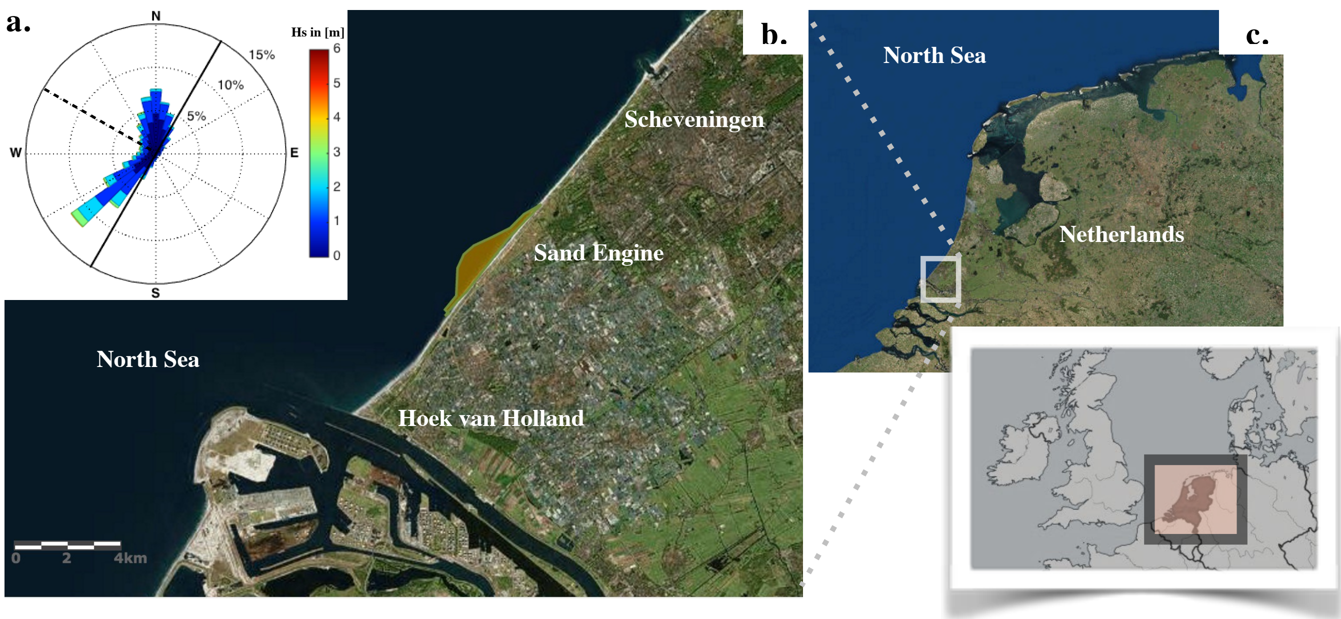

Figure 3.1. Location of the Sand Engine mega-nourishment on the southwestern coast of Holland between the harbour entrances of Scheveningen and Hoek van Holland (II) & (III). This 17 km stretch of coast (Westland coastal cell) is situated on the North Sea where the wave climate is considered to be wind-sea dominated with an annual mean wave height of 1.3 m and wave periods of 5-6 seconds (I).

The wave climate is considered to be wind-sea dominated with an annual mean wave height of 1.3 m and wave periods of 5-6 seconds. However, more energetic events are typical of the winter and autumn months with offshore waves in the order of 4 m approaching from the south and west sectors at highly oblique angles of incidence, which is very similar to the long term averaged wave climate (Wijnberg, 2002). The tidal range at the Sand Engine is approximately 1.7 m with horizontal tidal velocities reaching up to 0.5 m/s. These energetic conditions increase sediment stirring and transport along the perimeter of this nourishment inducing significant 3D features, especially in the intertidal zone.

Beach scarps are one of the most persistent features in this intertidal area at the Sand Engine. After its completion, the first scarps were observed from winter and spring of 2012 along the southern flank, head, and point. Furthermore, scarps have also been observed during calmer conditions; for instance, Shore Monitoring (2015) recorded scarps at the point of the Sand Engine during the summer of 2012 when the wave climate was rather calm.

Throughout this report, reference will be made to various spatial areas at the Sand Engine. To avoid any confusion, figure 3.1.b displays a general schematization of the Sand Engine and the spatial identifications used in this report.

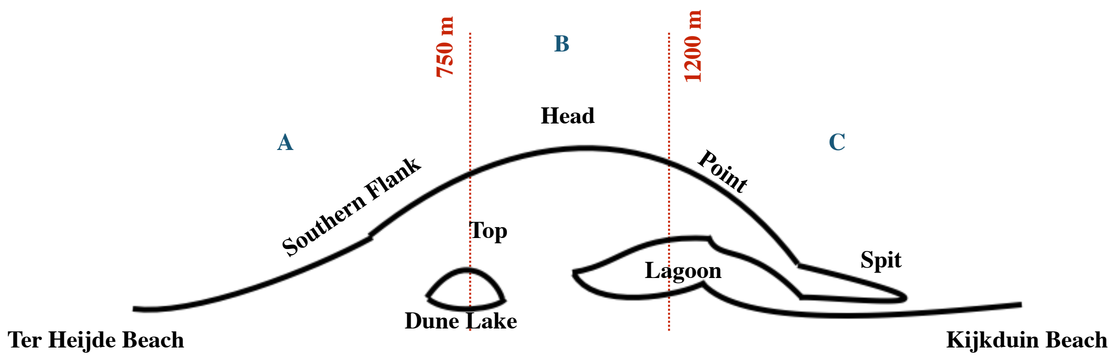

Figure 3.2. General schematization of the Sand Engine shape and the spatial terminology used in the remainder of the report (after Shore Monitoring 2013 & 2015). The cross-shore transects (red dotted lines) indicate the alongshore boundaries dividing the (A) 'southern flank' (B) 'head' & (C) 'point' along the perimeter of this mega-nourishment.

For more information on morphologic observations at the Sand Engine, one is referred to de Schipper et al. (2016) & Shore Monitoring (2013 & 2015).

3.2. Process Measurements

All process measurements described here were taken from Shore Monitoring (2013 & 2015).

This section will display different hydrodynamic recordings observed throughout the lifespan of the Sand Engine in an attempt to understand the processes which influence beach scarping. Furthermore, it will also yield insight to the extreme events of December 2013 & July 2015, considering these storms induced significant morphological change. A high energy event was deemed a "storm" based on the wind strengths recorded in Vlieland; to put this in perspective, there have only been 60 storms recorded from 1910 to present date. High energy waves (> 2 m) and increasing water levels near the shoreline due to surge are typical storm characteristics.

3.2.1. Hydrodynamics & Storm Conditions

The concurrent hydrodynamic conditions for each survey period were recorded from a wave station called the 'Europlatform', which is located 40 km offshore at a water depth of 32 m (de Schipper et al. 2016). The conditions measured consisted of significant offshore wave height ($H_{s,0}$), wave direction (θ_0), and wave period ($T_{m02,0}$). Furthermore, water levels ($\boldsymbol{\eta}$) recorded in the Scheveningen Harbour were also analyzed, particularly during storm events; the harbour helps to mitigate potential distortion in water levels due to wave action, which provided more accurate readings. Extreme weather conditions have the potential to heavily alter the cross-shore profile of sandy beaches, particularly scarps; as waves become more energetic, along with increasing water levels due to storm surge leaving new parts of the Sand Engine exposed to attack. The wave roses between each measurement period can be observed in Appendix D.

<u>December 5th, 2013 Storm</u>

The largest storm since the completion of the Sand Engine occurred on December 5th, 2013 (Northern Hemisphere Winter). The wind station at Hoek van Holland measured a maximum hourly average of 23 m/s with gusts of 35 m/s (Shore Monitoring, 2013). The highest water level recorded during the storm was 3.07 m above mean sea level with the largest offshore significant wave height being 5.1 m. In general, the dominant wave direction for the duration of the storm appeared to be relatively shore normal.

<u>July 25th, 2015 Storm</u>

This storm was not as severe as the one on December 5th, 2013, but was unusual for a summer event. Northwesterly wind speeds reached up to 22 m/s in the height of the storm, but did not last long. The maximum water level was 1.62 m above mean sea level with the largest offshore significant wave height being approximately 4.3 m.

Table 3.1 displays average and maximum values of the hydrodynamic recordings between each measurement period. This table will be referenced and discussed further in chapter 5 of this report.

Survey Period	Avg. $H_{s,0}$ [m]	Max $H_{s,0}$ [m]	Avg. $T_{m02,0}$ [s]	Max $T_{m02,0}$ [s]	Avg. η [m]	Max η [m]	Avg. (θ_0) [deg]	Storm [days]	High Waves [days]
Aug - Sep 2011	1.04	3.18	4.08	6.5	0.09	1.60	223	-	0
Sep - Oct 2011	1.38	4.13	4.34	6.7	0.13	1.60	228	-	6
Oct - Nov 2011	1.15	3.16	3.98	6.3	-0.02	1.50	184	-	0
Nov - Dec 2011	**1.78**	**5.59**	**4.66**	**7.5**	**0.21**	**2.43**	**237**	**1**	**11**
Dec - Jan 2012	2.18	5.13	5.21	7.1	0.27	2.30	266	-	7
Jan - Feb 2012	1.34	3.93	4.32	6.4	-0.12	1.99	201	-	3
Feb - Mar 2012	0.69	2.63	4.10	5.9	-0.13	1.56	243	-	0
Mar - Apr 2012	1.11	3.25	4.53	6.7	-0.06	1.53	213	-	0
Apr - May 2012	1.07	2.49	4.42	6.1	-0.05	1.38	229	-	0
May - Jun 2012	1.09	4.04	4.41	6.7	-0.02	1.43	183	-	2
Jun - Jul 2012	1.11	3.75	4.30	6.2	0.02	1.43	242	-	1
Jul - Aug 2012	0.70	1.78	3.79	5.9	-0.01	1.34	183	-	0
Aug - Oct 2012	1.31	4.80	4.37	6.9	0.12	1.74	251	-	1
Oct - Dec 2012	1.52	4.63	4.47	7.3	0.10	2.10	222	-	4
Dec - Feb 2013	1.47	3.70	4.39	6.6	0.00	1.82	198	-	7
Feb - Apr 2013	1.25	3.34	4.37	6.4	-0.17	1.43	123	-	1
Apr - Jul 2013	1.11	3.10	4.26	6.5	-0.04	1.53	206	-	0
Jul - Aug 2013	0.76	2.23	3.94	6.0	-0.02	1.36	186	-	0
Aug - Dec 2013	**1.38**	**5.33**	**4.36**	**7.5**	**0.10**	**2.04**	**224**	**1**	**7**
Dec - PS Dec 13	**2.10**	**4.89**	**5.24**	**7.2**	**0.37**	**3.07**	**295**	**1**	**2**
PS Dec - Feb 2014	**1.76**	**4.69**	**4.57**	**7.1**	**0.03**	**1.70**	**216**	**1**	**9**
Feb - Apr 2014	1.04	2.77	4.16	6.2	-0.05	1.65	203	-	0
Apr - Jun 2014	**0.88**	**3.59**	**4.27**	**6.4**	**-0.05**	**1.41**	**171**	**1**	**1**
Jun - Sep 2014	1.03	4.24	4.14	6.8	0.06	1.58	221	-	2
Sep - Oct 2014	**1.14**	**5.38**	**4.30**	**7.2**	**0.12**	**2.85**	**206**	**1**	**2**
Oct - Jan 2015	1.68	4.61	4.65	6.8	0.14	2.16	214	-	14
Jan - Mar 2015	1.35	4.39	4.39	6.8	0.00	2.02	241	-	4
Mar - Jun 2015	**1.13**	**4.26**	**4.31**	**6.7**	**-0.05**	**1.84**	**195**	**1**	**4**
Jun - Jul 2015	0.94	2.62	4.12	6.5	-0.04	1.45	206	-	0
Jul - Aug 2015	**1.29**	**4.33**	**4.45**	**6.7**	**0.09**	**1.62**	**237**	**1**	**1**
Aug - Sep 2015	1.10	3.58	4.13	6.5	0.06	1.62	206	-	1
Sep - Jan 2016	1.02	2.96	3.96	5.6	0.13	2.09	169	-	-

Table 3.1. Daily averages and maxima of the hydrodynamic conditions between each measurement period. Column 1 contains the measurement month and year. Columns 2 & 3 display the average and maximum significant wave heights between consecutive surveys. Columns 4 & 5 display the average and maximum wave periods respectively. Columns 6 & 7 contain the average and maximum water levels recorded in the Schevenengen Harbour. Column 7 displays the average wave direction between each survey. Finally, columns 8 & 9 display the storm and high wave (> 2 m) durations, respectively, in number of days. The rows in red denote periods where a storm was recorded. All wave data was recorded at the 'Europlatform'.

3.3. Morphology Measurements

All measurements described here were carried out by Shore Monitoring (2013 & 2015).

An intensive monitoring program was initiated upon completion of the Sand Engine in July 2011 and thoroughly described in de Schipper et al. (2016). Surveys of the beach and shoreface were conducted on a monthly basis in the first year after construction starting in August 2011, and semi-monthly beyond August 2012 through January 2016. The full surveys of this area are always carried out in approximately 4 days depending on the weather conditions.

Bed elevations were measured using three real-time kinematic differential global positioning system (RTK-GPS) survey techniques depending on spatial characteristics of the section being analyzed (e.g. subaqueous or subaerial). Subaqueous and subaerial sections were measured through use of a GPS mounted waverunner/jetski and 4WD quad bike, respectively. Narrow tidal channels and runnels were measured by attaching the GPS to a wheel pole, which was then manually rolled through shallow water. The vertical accuracy of these measurements are in the order of 10, 5, and 3 cm respectively (Huang et al. 2002; Ruggiero et al. 2009; van Son et al. 2010).

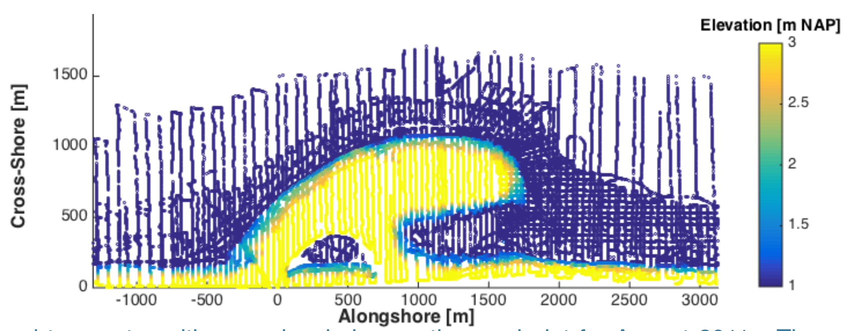

Figure 3.3. Surveyed transect positions on local shore orthogonal plot for August 2011. The reader can notice the variation in survey paths during the measurement period.

The survey domain consisted of 4.7 by 1.6 km in along- and cross-shore directions, with the cross-shore extent spanning from the dunefoot (+5 m NAP) to the —10 m NAP contour approximately. Each survey consisted of measuring the bottom levels along roughly fixed transects (see figure 3.3) and interpolated to develop bathymetric surfaces (see Appendix A). Also, in order to more easily analyze the morphodynamics of this mega-nourishment with respect to along- and cross-shore directions, the bed elevations were rotated to a local shore-orthogonal coordinate system (de Schipper *et al*. 2016).This was done by creating a matrix, which is used to perform a rotation in Euclidean space. To carry out this rotation, the position of each data point must be represented by a vector containing the x, y, and z coordinates of that particular point; furthermore, the desired rotated vector is obtained by using matrix multiplication (see figure 3.3).

Table 3.2 below is an overview of the survey periods in chronological order and the number of days that passed between them. Also, the reader should reference Appendix A for more detailed descriptions of what morphology was observed during each measurement period, along with bathymetric figures.

No.	Survey Month & Year	Time Lapse [days]
1	August 2011	-
2	September 2011	30
3	October 2011	41
4	November 2011	28
5	December 2011	45
6	January 2012	18
7	February 2012	42
8	March 2012	24
9	April 2012	36
10	May 2012	26
11	June 2012	24
12	July 2012	34
13	August 2012	27
14	October 2012	46
15	December 2012	68
16	February 2013	61
17	April 2013	66
18	July 2013	67
19	August 2013	50
20	December 2013	102
21	Post-Storm December 2013	6
22	February 2014	70
23	April 2014	60
24	June 2014	64
25	September 2014	71
26	October 2014	54
27	January 2015	81
28	March 2015	50
29	June 2015	82
30	July 2015	42
31	August 2015	16
32	September 2015	51
33	January 2016	103

Table 3.2. Overview of measurement periods discussed in this report. Column 1 displays the survey number, where there are 33 in total. Column 2 displays the month & year of the recordings. Finally, Column 3 displays the amount of time that passed between each survey.

3.3.1. Limitations

Survey measurements were taken during calm conditions at low tide in order to make the intertidal region more accessible for the surveying equipment. Seeing as though beach scarps in the area range anywhere from 15 cm to almost 2 m, the 4WD quad-bike could not roll over the larger-steep edges. To mitigate this effect, the quad bike was driven close to the edge from both directions on the upper and lower beach. However, this presents a resolution issue when identifying these features which have such an abrupt change in profile gradient. The gap between the final measurement on the upper beach and the first point on the lower beach is approximately 5 m for the larger scarps (in the order of 1 - 2 m). Part of the reason for this significant gap is due to the notching of the scarp face, leaving large mounds of sand at its base (solid red line in figure 3.4). Also, the quad bike cannot approach the edge too closely without the scarp collapsing, which forces the survey crew to stop short of a desired location at times. Furthermore, from analyzing the raw survey tracks at a higher resolution, it seems as though some scarps of smaller magnitude (order of 15 - 25 cm) were simply rolled over with the surveying equipment.

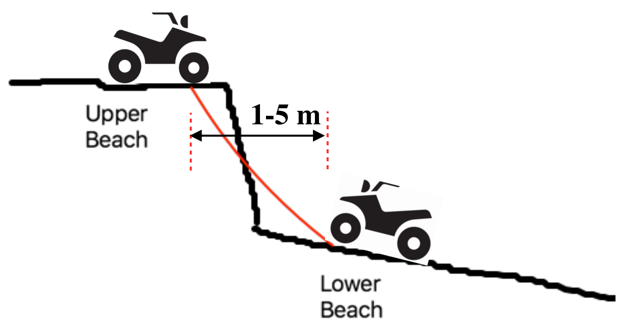

Figure 3.4. Schematization demonstrating the measurement limitations when surveying beach scarps with the 4WD quad bike.

With all of this in mind, the next step in this research phase was to create an automated method/tool which would simultaneously evaluate every survey period and extract these features from the original dataset for further assessment of evolutional patterns.

3.4. Beach Scarp Identification

A semi-monthly survey dataset taken by Shore Monitoring at the Sand Engine was analyzed in an attempt to identify beach scarps along the peninsula. The dataset consisted of bed elevations for 33 different survey periods spanning from August 2011 to January 2016. Among many characteristics, scarp initiation and persistence were especially of interest because this will aid in future predictive skill. The scarp identification method used in this project was taken from Ruiz de Algria-Arzaburu et al. (2013) and validated with manual transect analysis of the raw data.

3.4.1. Automated Identifier

In an attempt to automate the scarp extraction process for more efficient analysis, a script/tool was created using Matlab software. Figure 3.2. demonstrates the geometry of the survey paths, which roughly follow the same lines for each survey period; however, not exact. Based on this, the spacing between the raw data paths was more closely examined to determine an adequate transect spacing.

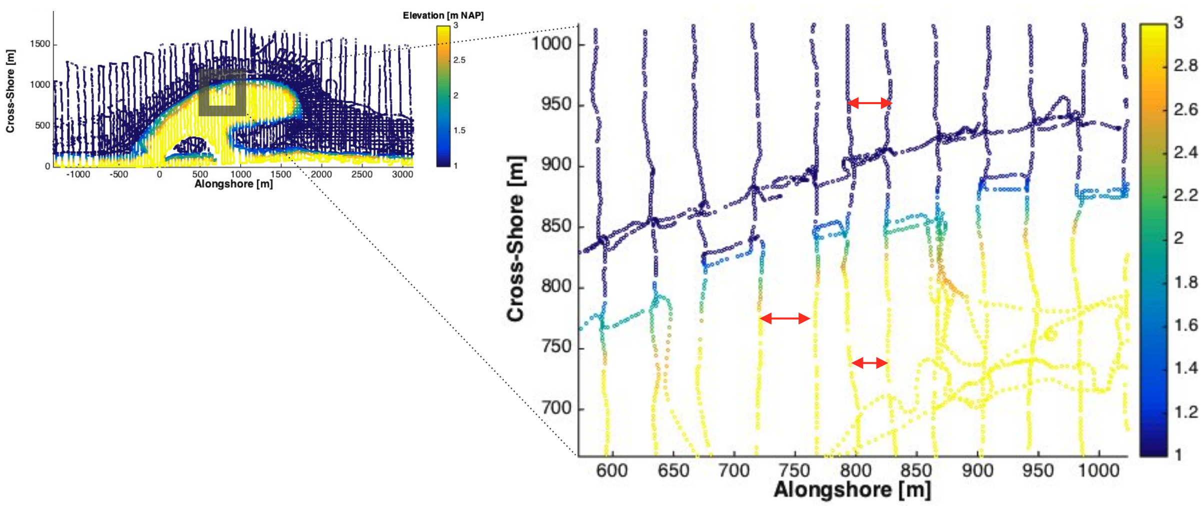

Figure 3.5. Close up of raw data points and survey pathways for August 2011 measurements. The red arrows are intended to demonstrate how the spacing varies so fixed transects may not fall directly on the data points.

After examination of the tracks, 35 transects of 575 m in length were implemented at a fixed spacing of 35 m spanning from the 400 m alongshore position to the 1590 m alongshore position. Also, the transect was filtered to only show the areas above 0 m NAP (subaerial). In order to attain nearly 1 m resolution, the raw data points were interpolated to 500 grid points along each transect. One disadvantage of increasing the number of grid points was that it tended to produce more ‘noise’ in the differentiation results, which was causing the crest to be picked up at a point higher in the profile than it actually was. However, a conditional statement to further filter the data was implemented to mitigate this effect.

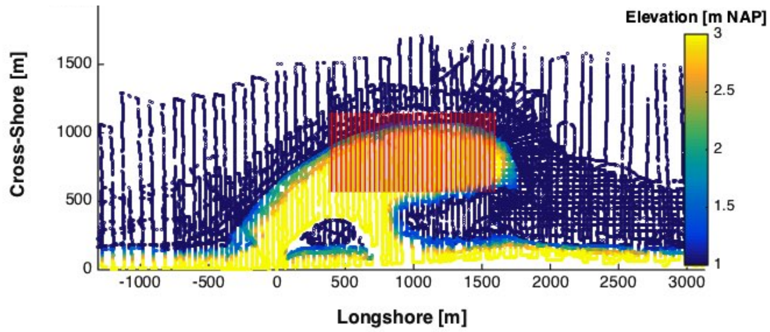

Figure 3.6. Shore orthogonal plot of the raw data points taken at the Sand Engine. The 35 red lines represent the transect locations along the edge of the peninsula.

The Matlab script was generated such that 35 transects could be evaluated simultaneously for all 33 measurement periods, producing the locations and approximate heights of every scarp identified. The method used to identify the scarps was taken from Ruiz de Algria-Arzaburu et al. (2013), where the scarp crest and toe were identified by the local minimum and maximum of the second order derivative, respectively.

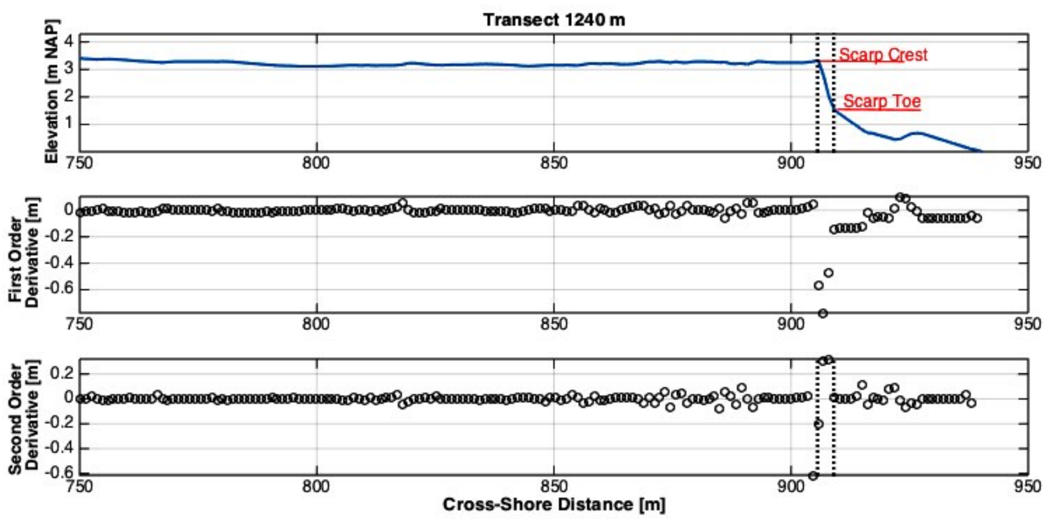

Figure 3.7. Scarp extraction tool. (top) transect 31 of the 35 transects at alongshore position 1240 m. (middle) First order derivative of the transect elevations (bottom) second order derivative of the transect elevations; black dotted lines indicate the minimum and maximum of the second order derivative and are also placed in the top figure to show the scarp crest and toe locations respectively.

The tool starts by making use of the first order derivative to identify the largest difference in elevation between consecutive data points along the transect profile. In other words, the elevations of consecutive data points were differentiated Next, it takes the second order derivative of said profile in order to obtain the largest difference in elevation once again. It could be argued that the first derivative would suffice in locating the scarp crest, but implementing the second order derivative proved more accurate in locating the upper beach edge.

Once the crest and toe locations were obtained, the tool then goes on to calculate the slope and height of the scarp face. Ruiz de Algria-Arzaburu et al. (2013) deemed a scarp to be any feature larger than 25 cm with a slope greater than the critical angle of repose (32 degrees). For the sake of this report, a scarp was taken to be any feature larger than 30 cm with a slope greater than or equal to 0.15. The justification for these criteria will be explained in more detail in the following sections.

3.4.2. Manual Identification

Shore Monitoring conducted the surveys at the Sand Engine analyzed in this report, and recorded first order scarp observations during each measurement period. The authors observations for each survey period are briefly described in Appendix A. These observations, along with the recorded bed elevations, were utilized in an effort to validate and add to the automated tool described in section 3.4.1.

The raw survey data was used instead of a gridded bathymetry throughout the analysis process, which was due to the idea that more accurate measurements would come from the recorded bed elevations rather than an interpolated surface. However, as previously demonstrated in section 3.4.1., the survey pathways varied spatially from one survey to the next. Therefore, each survey was manually analyzed at a higher resolution to identify areas where the 'usual' pathways were strayed from (or 'cut-short'), which would be an indicator for a scarp due to the measurement restrictions mentioned in section 3.3.1.

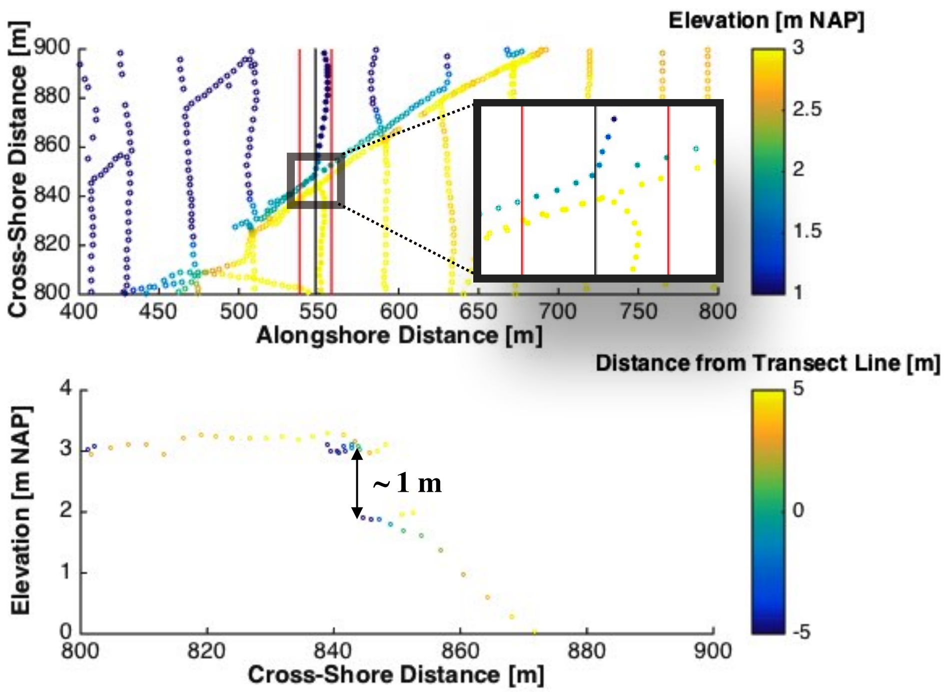

Figure 3.8. (Top) Magnified look at the survey paths from August 2012 : Survey #13. The black line is a Manually input transect with a 10 m buffer (red lines) on either side. (Bottom) Profile view of transect 548 m. The reader should notice the gap between data points at +3 m NAP and +2 m NAP. This gap was presumed a scarp during data analysis.

Once these areas were identified, transects were manually fit to the raw data points so that each transect line intersected as many points as possible in the cross-shore direction. A 10 m buffer was placed on either side of the manually input transect, which excluded any data points outside this region, to mitigate the inconsistency in survey tracks. Viewing the transect profiles confirms the measurement uncertainties explained in figure 3.4, due to the large gap between data points between +2 and +3 m NAP respectively. This process of identifying patterns similar to that of figure 3.8. was repeated for each survey period, and recorded to a database consisting of all identified scarps and their corresponding transect.

4. Results

This chapter will go on to display the results based on the methodology discussed in Chapter 3 of this report. It will begin by demonstrating the validation process of the scarp identification methods implemented, and justify the chosen criteria. Furthermore, it should provide a clear indication of beach scarp existence at the Sand Engine and give semi-quantitative insight on the morphologic change between surveys with respect to hydrodynamic conditions.

4.1. Method Validation

Figure 4.1 in this section shows where the automated tool identified a scarp (colored dots) compared to ones manually observed through the raw survey paths (black dots). Furthermore, various combinations of slope and height were implemented into the automated script, yet only brief results of varying slopes are demonstrated here.

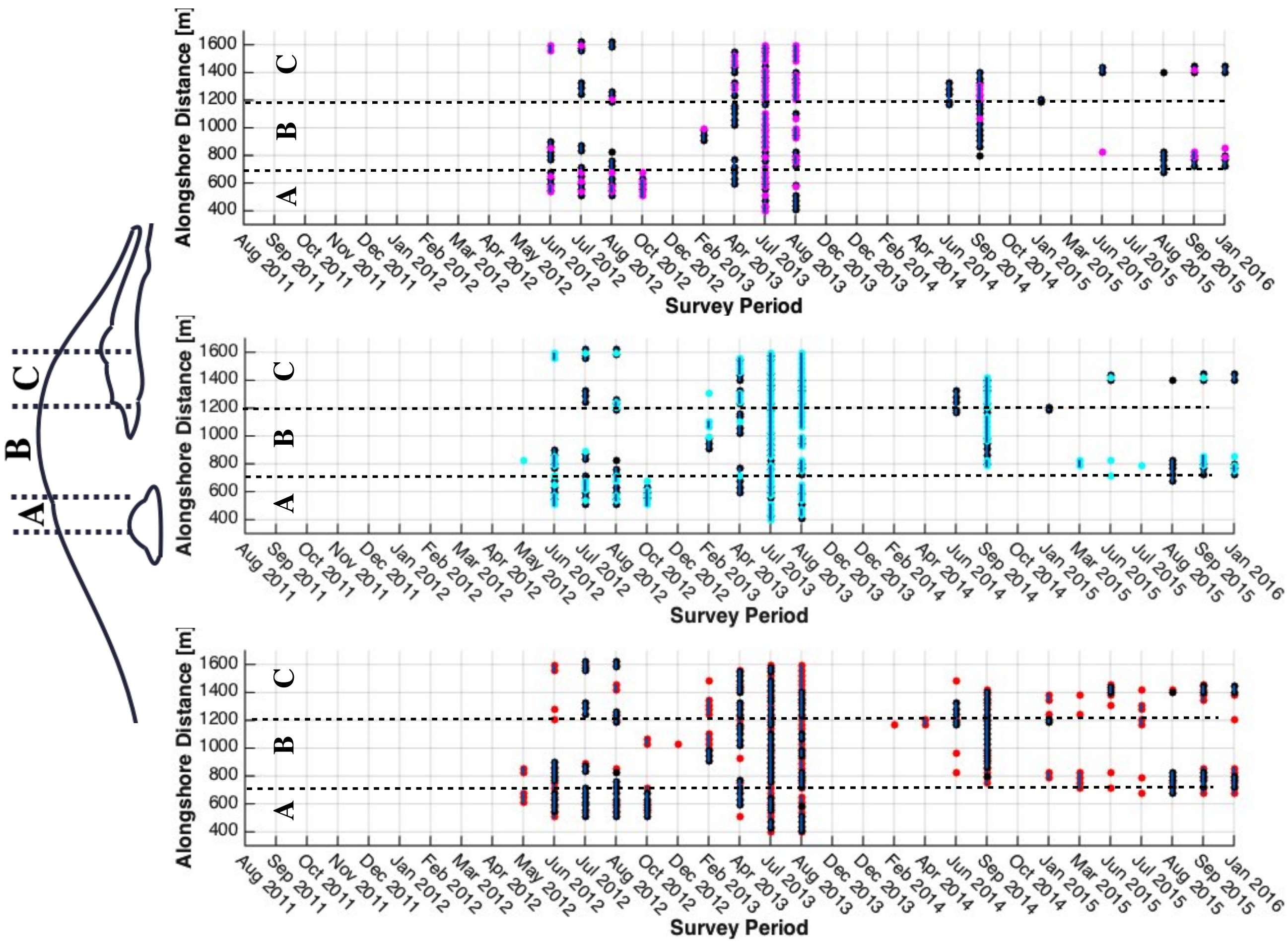

Figure 4.1. Binary existence plots demonstrating the validation of the automated tool with respect to Raw data Observations. the slope criteria implemented were 0.20 (top) , 0.15 (middle), & 0.10 (bottom) respectively. Black points in all three figures represent the scarps identified through manual transect analysis.

The middle existence plot in figure 4.1 implements a minimum slope and height of 0.15 and 30 cm respectively, and was ultimately chosen as the best criteria fit; considering the automated results and raw data observations have the most overlap. Furthermore, neither method identifies a scarp for the first 10 survey periods, no matter the conditional statement implemented for height and slope. Decreasing the minimum height and slope requirements only added more noise to the existence plots (see figure 4.1-bottom) and decreased the accuracy. Therefore, to maintain the integrity of the results, the required criteria was kept the same.

4.2. Database

A database was created including all identified beach scarps at the Sand Engine using the automated tool described in section 3.4.1, and manual transect analysis described in section 3.4.2. The results shown in the sections below are intended to give an overall summary for how beach scarp existence varies in space and time at the Sand Engine.

4.2.1. General Observations

All manually identified scarps were taken into consideration in this section as they were the most certain scarp observations. Behavioral differences in beach scarping, depending on spatial and temporal variation at the Sand Engine, can be observed from figure 4.2. The tables in Appendix B display the alongshore transect positions of each located scarp in the database.

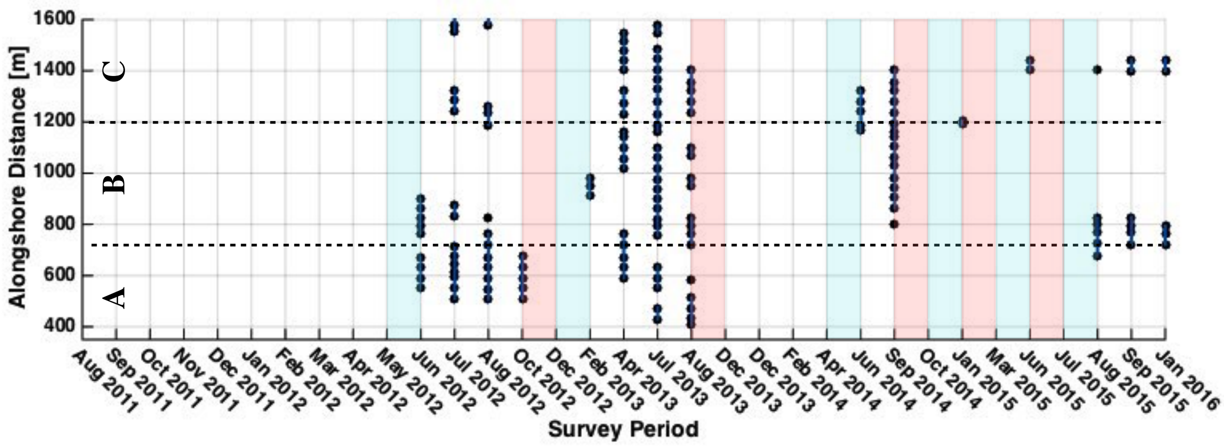

Figure 4.2. Binary existence plot demonstrating the scarps confirmed through manual identification described in section 3.4.2. The blue and red shading represents periods of scarp creation and removal respectively.

<u>The 'Southern Flank'</u>

Scarp existence at the southern flank appears to be less common than at the head and point, particularly after August 2013. They were fairly persistent between periods June 2012 and October 2012 in this area; however, it is interesting to note that all scarps disappeared by December 2012. The following recordings of July 2013 and August 2013 showed scarps spanning most of the southern flank; the locations seem to remain constant between these two periods, suggesting scarp preservation between measurements. Beyond December 2013, scarps only existed during the August 2015 measurements at the southern flank, which is approximately 2 years after the previous recordings.

<u>The 'Head'</u>

Beach scarp existence appears quite frequent at the head of the Sand Engine. The first scarps were observed at the head in June 2012 through the August 2012 measurements. The automated tool picks up a scarp prior to these measurements in May 2012 (see figure 4.1), but this was disregarded considering no scarp was detected during the manual transect analysis described in section 3.4.2. Throughout these measurements, the number of scarps seemed to decrease linearly, merging towards the southern flank until they disappeared from the head completely (see figure 4.2).

Scarping at the head was observed again in February 2013 and existed rather regularly until the period of December 2013; July and August 2013 were the two measurement periods where the largest number of scarps were identified, yet interestingly enough, they do not appear at all the following month because they were not identified through either method; Reset periods such as this are of particular interest, when it comes to coupling the process controls to the resulting morphology (i.e. there must be a reason for the complete destruction of scarps spanning the entire perimeter).

Following the post-storm December 2013 measurements (7 days after previous December measurements), no scarps existed through April 2014. Scarps are observed again in June 2014 closer to the boundary line between the head and point (1200 m); however, the following measurements of September 2014 show scarps spanning along most of the perimeter at the head, which indicates scarp initiation mechanisms were present between measurements.

Beach scarps demonstrate an interesting pattern at the head during the final six surveys, where there appears to be persistent scarps near the boundary between the head and southern flank (750 m transect).

The 'Point'

Beach scarps were first observed at the point in June 2012 (Northern Hemisphere summer), and were persistent through the August 2012 measurements. They seemingly disappeared at the point during the October 2012 measurements, along with the scarps at the head indicating a reset event of some sort.

They appear on a consistent basis at the point from April 2013 to August 2013 spanning the majority of the perimeter of the Sand Engine. They disappeared at the point again after the winter storm of December 2013, and did not reappear until the summer of 2014 (June & September). Scarping at the point beyond these measurements became less frequent and more intermittent; this period is especially of interest because of the persistency observed between measurements.

4.2.2. Height Specifications

Figure 4.3 below shows the results of the automated tool only. This was done in order to examine trends in scarp height at the Sand Engine. The approximate scarp height and slope was calculated by taking the difference in elevation between the located crest and toe of the scarp. However, considering the measurement limitations discussed in chapter 3, it is important to note these scarp specifications may be over- or underestimated in some cases.

From figure 4.3, one can see the point of the Sand Engine appears to have scarps of the largest height, especially between the April and August 2013 measurement periods. It is also interesting to note the longshore color variability observed between said survey periods, indicating variations in scarp height.

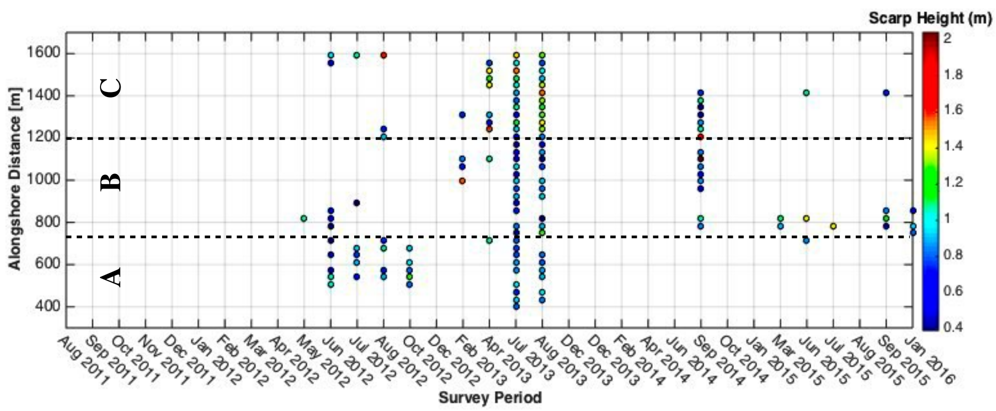

Figure 4.3. Binary existence plot demonstrating all scarps identified by means of the automated tool with fixed transect spacing of 35 m. The color of each point represents the approximate scarp height recorded along that particular transect.

The average scarp height over the entire 4.5 year duration was calculated along the perimeter of the Sand Engine with respect to each longshore boundary indicated in figure 4.3 above; the mean height at the southern flank, head, and point were 85 cm, 78 cm & 100 cm respectively. The mean scarp slope and heights are demonstrated in Table 4.1 below.

	Southern Flank	Head	Point
Mean Scarp Height [m]	0.85	0.78	1.0
Mean Scarp Slope	0.21	0.21	0.22

Table 4.1. Mean scarp height and slope over the entire 4.5 year monitoring period with respect to alongshore position.

4.2.3. Foreshore Slopes

Figure 4.4 below shows once again the results of the automated tool only; however, the coloration in data points represents the foreshore slope calculated between the scarp toe (~ 2 m NAP) and -1 m NAP, rather than the scarp height. These particular elevations were chosen due to the hypothesis that scarping only occurs when the water levels are at least 1 m above NAP. Therefore, the scarp toe to -1 m NAP was deemed as a good representation of the foreshore slope.

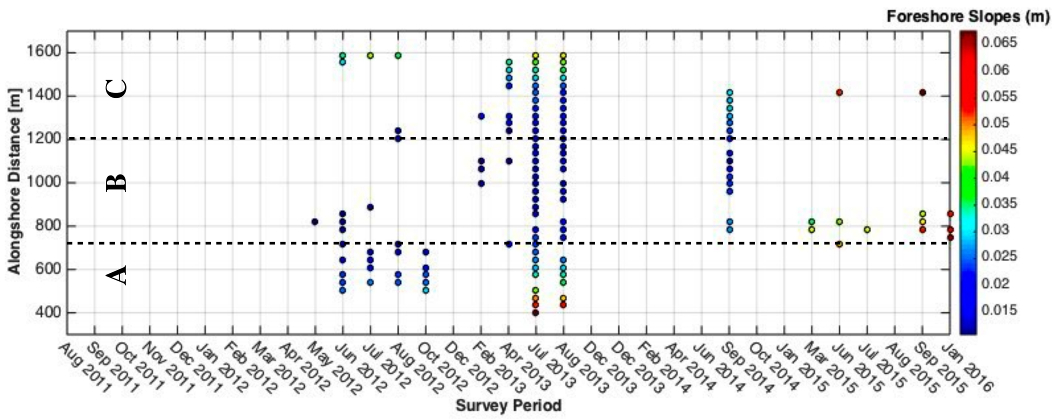

Figure 4.4. Binary existence plot demonstrating all scarps identified by means of the automated tool with fixed transect spacing of 35 m. The color of each point represents the foreshore slope recorded along that particular transect between the scarp toe (~ 2 m NAP) and -1 m NAP. -2 m NAP was also assessed, but the results did not vary significantly.

The foreshore slope calculations consistently yielded values between 1:20 and 1:50. The foreshore slope appears to be larger at the southern flank and point in comparison to the head; however, as the shape of the Sand Engine adjusted, the slopes along the head appear to increase especially after September 2014. The state of the foreshore profile is vital to understanding the nearshore energy regime and response of any coastline. Slope and nearshore bedforms (e.g. sandbars) determine the locations and rates of energy dissipation due to wave breaking, which influences the resulting runup. The mean foreshore slopes are demonstrated in Table 4.2 below.

	Southern Flank	Head	Point
Mean Foreshore Slope	0.035	0.021	0.030

Table 4.2. Mean foreshore slopes over the entire 4.5 year monitoring period with respect to alongshore position.

4.3. Subaerial Profile Evolution

This section will focus on analyzing a few representative transects at selected time periods in an attempt to better see how the profile changes and scarps develop along the perimeter of the Sand Engine. The time periods and transects were selected based on beach scarp persistence (see figure 4.2). Also, scatter plots showing correlation between scarp recession and hydrodynamics is displayed in Appendix D.

4.3.1. The Southern Flank (Transect 575 m)

May 2012 - Dec 2012

The figure 4.5 below demonstrates the profile along the 575 m transect line (southern flank) from May 2012 to December 2012. The profile was relatively smooth in May (figure 4.5, dark blue line); however, the lower part of the profile seems to be slightly eroding causing the cross-shore surface to become more concave with respect to the incoming waves. The geometry is similar to that of profile A in section 2.8.1; with the erosion of the lower intertidal, and the natural construction of a berm due to swash motions.

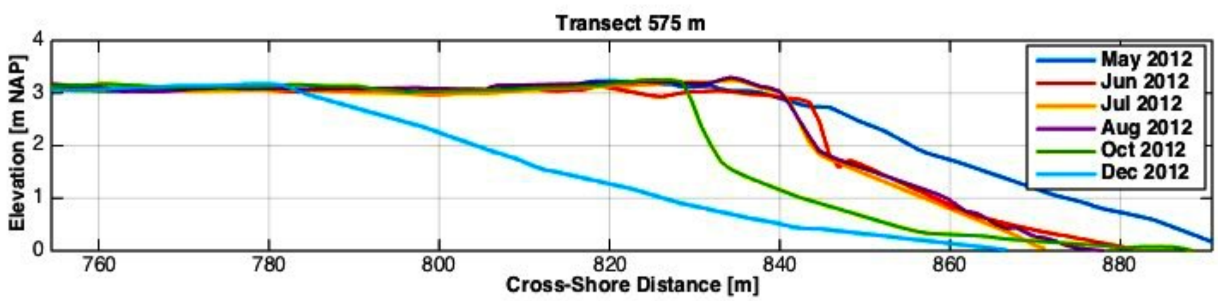

Figure 4.5. Transect 575 m from May 2012 to December 2012. The reader should notice the developed scarp from the June 2012 measurements through October 2012. By December 2012, the scarp appeared to be completely washed away.

By June 2012 (figure 4.5, red line), a scarp developed along this profile between the cross-shore distances of 820 - 850 m at approximately +1.5 - 2.8 m NAP. The upper beach edge has receded landwards about 2 m and is now referred to as the scarp crest, with the toe being situated at approximately the same cross-shore distance as the previous upper beach edge. It is also interesting to note that the upper beach edge (now scarp crest) has a higher elevation than that of the previous measurement period by 10 cm, insinuating some kind of onshore directed transport.

The scarp from the previous measurement period still remained in July 2012 (figure 4.5, orange line) with the scarp crest about 20 cm higher than before; the toe elevation has also increased by about 20 cm. Furthermore, the crest and toe receded 3 m and 2 m respectively from their previous positions.

Only slight profile changes were observed by August 2012 (figure 4.5, purple line), indicating the conditions were relatively moderate and the water levels may not have been high enough to reach the base of the scarp. Furthermore, the lower part of the profile seems to have adjusted itself to the same position as June 2012 (2 periods before). The crest has remained in the same position leaving the toe and lower intertidal positions as the only changing characteristics; the lower intertidal appears to have increased in elevation by as much as 7 cm.

Drastic change in morphology was observed from August 2012 (figure 4.5, purple line) to October 2012 (figure 4.5, green line). The scarp crest and toe have receded landwards once again by 10 m; the lower part of the profile has been eroded into a concave shape steepening the scarp face and increasing the height.

A general trend of increasing scarp height with increasing landward recession is observed up to this point; however, the scarp completely disappeared by December 2012 (figure 4.5, light blue line). The upper beach edge was measured at a cross-shore distance of 782 m yielding a 45 m difference from the previous measurements. The entire profile has been smoothed over and looks similar to that of the May 2012 profile, only further landwards.

4.3.2. The Head (Transect 1030 m)

<u>**Dec 2012 - Post Storm Dec 2013**</u>

Figure 4.6 below displays the profile along the 1030 m transect line from December 2012 to December 2013. The profile in December 2012 (figure 4.6, dark blue line) was fairly steep between elevations +1 to + 3 m NAP, with relatively flat intertidal slope below +1 m NAP.

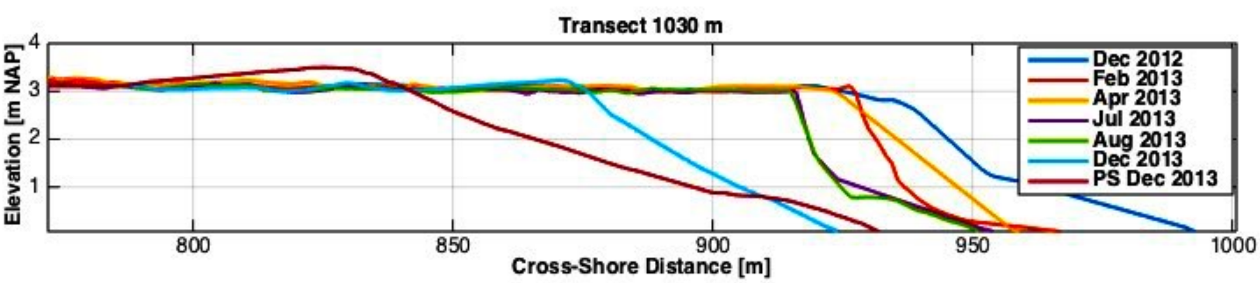

Figure 4.6. Transect 1030 m from December 2012 to December 2013. The reader should notice the developed scarp from the February 2013 measurements, which disappeared by April 2013. A scarp reappears in July 2013 and remains until December 2013.

The February 2013 (figure 4.6, red line) measurements indicated a large steepening of the profile leading to the development of a scarp. Furthermore, the upper beach edge (now scarp crest) has receded nearly 10 meters in the landward direction, along with a 20 cm increase in elevation. The profile appears more concave with respect to the incoming waves indicating severe erosion since the last measurement period. By April 2013 (figure 4.6, orange line), the scarp had disappeared leaving the upper foreshore with a relatively steep, but smooth slope. Interestingly enough, the resulting shape is similar to that of

December 2012 (figure 4.6, dark blue line) with a landward and downward shift of the profile. The scarp crest during these measurements receded landward by about 5 m, which is not nearly as drastic as the following period.

A scarp has reappeared in the profile during the measurements of July 2013 (figure 4.6, purple line) with the scarp crest being located nearly 10 m landward of the previous upper beach edge measurement. The profile has again become more concave, resulting in a shape similar to that of February 2013 (figure 4.6, red line). This scarp existed during the August 2013 (figure 4.6, green line) measurements as well, with a very similar shape to that of the previous period; the only difference being that the base of the scarp has been eroded slightly steepening the scarp slope and increasing the height.

By December 2013 (figure 4.6, light blue line), the scarp has completely disappeared leaving a relatively smooth slope behind. Once again, there was a 20 cm increase in the elevation of the upper beach edge, along with a landward recession of nearly 40 m. This is significantly larger than previous measurements indicating the probability of a high energy event between surveys.

Seven days later, measurements were taken again following a severe winter storm in an attempt to isolate the effects on the cross-shore profile (figure 4.6, dark red line). Once again, there was a landward shift of 40 m of the upper beach edge with a 30 cm increase in elevation. The profile appears to have a similar shape to that of the previous measurement period, with the only differences being a milder foreshore slope and what appears to be an intertidal sandbank in the lower profile.

4.3.3. The Point (Transect 1240)

<u>Apr 2013 - Feb 2014</u>

Figure 4.7 below demonstrates the profile along the 1240 m transect line from February 2013 to December 2013. The slope of the profile between the upper beach edge and the lower intertidal was relatively steep (1:10) along this transect during the February 2013 measurements (figure 4.7, dark blue line), but no scarp had yet developed.

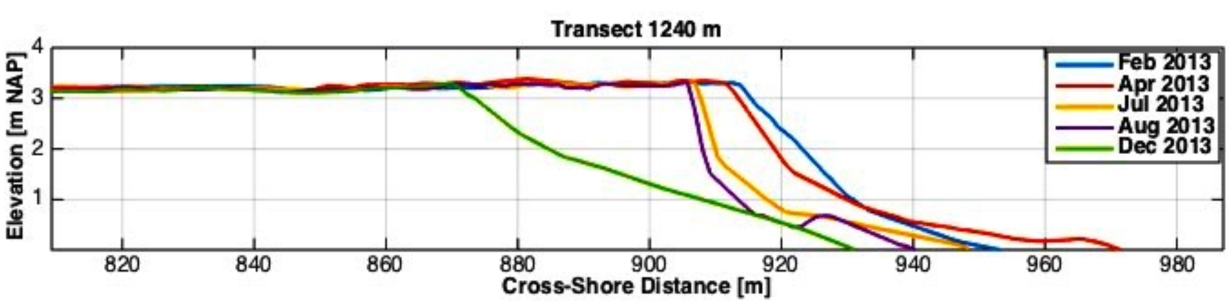

Figure 4.7. Transect 1240 m from February 2013 to December 2013. The reader should notice the developed scarp from the April 2013 measurement period, which remained until December 2013.

A scarp was observed during the April 2013 measurements (figure 4.7, red line) as the face of the profile continued to steepen. There appears to be deposition in the lower profile, whereas the upper beach edge receded 2 m in the landward direction.

The scarp from the previous measurement period was again observed in July 2013, but at a more landward position; the crest of the scarp had receded approximately 6 m; also, the profile has increased in concavity causing the upper profile to become steeper.

The profile only slightly changed between July and August 2013, with the crest remaining approximately in the same position; the only difference appeared to be the slight increase in elevation of the sandbank in the intertidal, along with the formation of a runnel ('zwin') just seaward of the scarp face. The concavity of the profile has again increased.

Following the storm of December 2013, the profile measurements showed that the scarp had been destroyed leaving a rather mild slope behind. The upper beach edge receded 35 m landward.

4.3.4. Reset Event

Oct 2012 - Dec 2012 (505, 540, 575, 610 & 680 m)

Two survey periods were isolated along with the hydrodynamic recordings between them; measurement periods 14 & 15 (Oct & Dec 2012) were chosen for evaluation because of the significant change between surveys. Scarps were observed along 5 transects during the October 2012 measurements along the southern flank (see figure 4.8); Transects 505, 540, 575, 610 & 680 m had scarp crest (S_{HI}) elevations of 3.0, 3.2, 3.1, 3.0 & 3.0 m respectively. By the December 2012 measurements (68 days later), all five scarps had been completely washed away indicating a possible increase in the nearshore energy and water levels during the lapse in surveys.

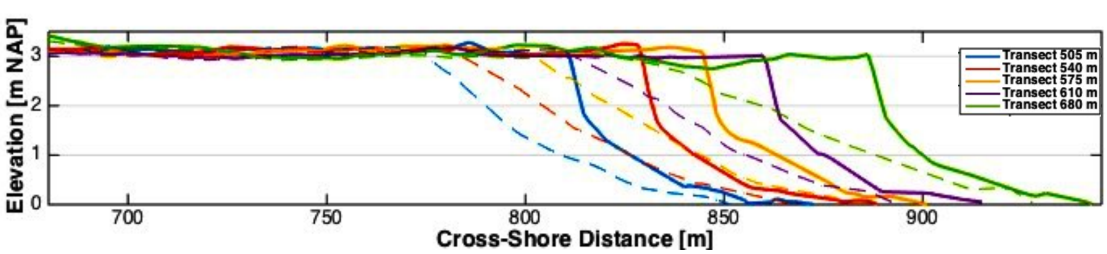

Figure 4.8. Consecutive transects (505, 540, 575, 610 & 680 m) at the southern flank of the Sand Engine during the October 2012 measurements (solid profile lines); the same transects 68 days later in December 2012 (dotted profile lines).

As previously mentioned, reset events such as this are of particular interest seeing as it has the potential to yield insight on the mechanisms influencing these cliff-like formations. It is also interesting to note that the automated tool picked up scarps along 4 consecutive transects at a 35 m alongshore spacing (505, 540, 575, 610), yet another was not located until the 680 m transect line (green profile). This indicated there is a break of some sort in the longshore extent of beach scarping during this period and reinforces the alongshore variability described by Seymour et al., (2005).

This section has displayed multiple figures demonstrating profile development and pointed out the noteworthy characteristics within each. The following section 4.4 will discuss these results in more detail and attempt to derive delineations between process and form.

4.4. Framework Validation

In an effort to validate the beach scarp observations and the hypothesized regime framework described in Chapter 2, this section will display approximate runup values based on the equations in section 2.5.2. The framework was tested using scarp crest elevations along the 1100 m transect. The approximate run-up and rundown values (R_{HI}) and (R_{LO}) were calculated based on maximum water levels and wave conditions between each measurement period. The cross-shore slope was calculated between the +2 m to -1 m NAP elevations, which consistently yielded a value between 1:20 & 1:50. Bearing all these assumptions in mind, these parameters were then compared to scarp existence at the Sand Engine in an effort to better understand the process controls. The results of this framework validation are displayed in figure 4.9 & table 4.2 below.

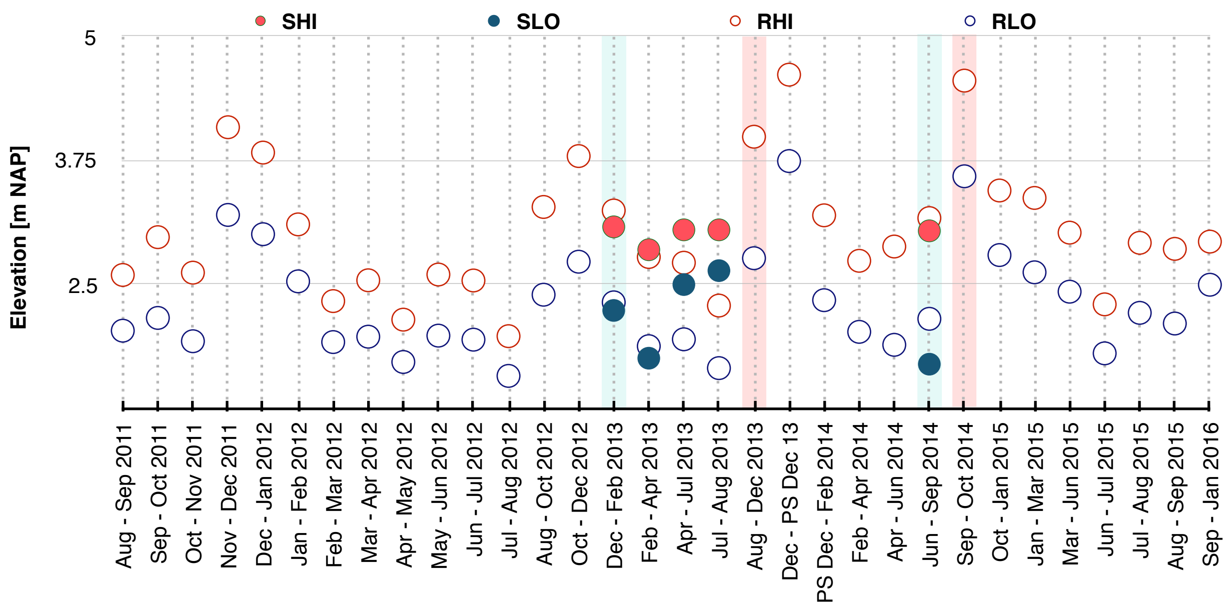

Figure 4.9. Scarp crest (S_{HI}) and toe (S_{LO}) elevations [m NAP] in time versus high (R_{HI}) and low (R_{LO}) runup approximations. Formulas used to derive runup values are displayed in Chapter 2, and taken from Holman (1986) & Sallenger (2000). The blue and red shading denotes periods of scarp creation and removal respectively.

A scarp was first observed along the 1100 m transect during the February 2013 measurements (see figure 4.9 - solid red circles). The maximum water level recorded in the 61 day time lapse between surveys was 1.8 m NAP, with the resulting R_{HI} at 3.24 m. This scarp creation period is indicated by the blue shading in figure 4.9, and the resulting scarp characteristics (S_{HI} & S_{LO}) were 3.08 m and 2.24 m respectively.

The scarp crest elevation lowered by the following measurement period (April 2013) and was situated at an elevation of 2.85 m NAP. The runup indicates the collision regime was reached in the 66 day time lapse, where R_{HI} was calculated at 2.78 m. The collision of the runup with the scarp face may explain the deterioration of the scarp crest; however, the scarp height appeared to increase from 84 cm to 1.09 m.

The scarp was again observed during the July 2013 measurement period with the crest and toe at elevations of 3.05 and 2.5 m NAP respectively; the crest elevation is similar to that of the original observation; however, the scarp height decreased to 55 cm. R_{HI} and R_{LO} were found to be 2.72 m and 1.95 m respectively, which indicates the scarp reached the collision regime once again.

The scarp crest remained in the same position (3.05 m) by the following period (August 2013), but the toe appeared at a higher elevation decreasing the scarp height by 14 cm. This decrease in height was unexpected considering R_{HI} never reached the scarp toe, indicating the swash regime (2.29 m < 2.50 m). Explanations for this unexpected observation will be further addressed in Chapter 5.

The scarp along the 1100 m transect line was removed by December 2013 (figure 4.9 - red shading). However, this finding was expected as R_{HI} surpassed the scarp crest by approximately 90 cm. R_{LO} was found to be approximately 2.77 m, which is about 30 cm lower than the previous crest recording. Therefore, it appears the overtopping regime led to scarp removal.

A scarp was again observed during the September 2014 measurement period with S_{HI} and S_{LO} at 3.04 m and 1.7 m respectively. R_{HI} and R_{LO} were approximately 3.17 m and 2.16 m NAP respectively, between June and September 2014; the maximum water level during this time frame was 1.5 m NAP. These conditions which describe this creation period are similar to the conditions of December 2012 to February 2013. The scarp disappeared by the following measurement period (October 2014) upon entering the inundation regime. R_{HI} and R_{LO} reached 4.55 m and 3.59 m NAP respectively, completely submerging the scarp. These large runup magnitudes are attributed to a storm that was recorded between measurement periods. Table 4.3 on the following page is intended to give the reader a more clear depiction of the values observed in figure 4.9.

Survey Period	**R_{HI} [m]**	**R_{LO} [m]**	**S_{HI} [m]**	**S_{LO} [m]**	**Regime**
Aug - Sep 2011	2.60	2.04	-	-	-
Sep - Oct 2011	2.98	2.16	-	-	-
Oct - Nov 2011	2.62	1.93	-	-	-
Nov - Dec 2011	4.08	3.20	-	-	-
Dec - Jan 2012	3.83	3.01	-	-	-
Jan - Feb 2012	3.10	2.53	-	-	-
Feb - Mar 2012	2.33	1.92	-	-	-
Mar - Apr 2012	2.54	1.98	-	-	-
Apr - May 2012	2.15	1.72	-	-	-
May - Jun 2012	2.60	1.99	-	-	-
Jun - Jul 2012	2.54	1.95	-	-	-
Jul - Aug 2012	1.98	1.58	-	-	-
Aug - Oct 2012	3.28	2.40	-	-	-
Oct - Dec 2012	3.79	2.73	-	-	-
Dec - Feb 2013	3.24	2.32	3.08	2.24	creation
Feb - Apr 2013	2.78	1.88	2.85	1.76	collision
Apr - Jul 2013	2.72	1.95	3.05	2.50	collision
Jul - Aug 2013	2.29	1.66	3.05	2.64	swash
Aug - Dec 2013	3.99	2.77	-	-	removal / overtopping
Dec - PS Dec 2013	4.61	3.74	-	-	-
PS Dec - Feb 2014	3.20	2.34	-	-	-
Feb - Apr 2014	2.74	2.02	-	-	-
Apr - Jun 2014	2.88	1.89	-	-	-
Jun - Sep 2014	3.17	2.16	3.04	1.7	creation
Sep - Oct 2014	4.55	3.59	-	-	removal / inundation
Oct - Jan 2015	3.45	2.80	-	-	-
Jan - Mar 2015	3.37	2.62	-	-	-
Mar - Jun 2015	3.02	2.43	-	-	-
Jun - Jul 2015	2.30	1.81	-	-	-
Jul - Aug 2015	2.92	2.22	-	-	-
Aug - Sep 2015	2.86	2.11	-	-	-
Sep - Jan 2016	2.93	2.50	-	-	-

Table 4.3. Scarp crest (S_{HI}) and toe (S_{LO}) elevations along the 1100 m transect versus high (R_{HI}) and low (R_{LO}) runup approximations. Formulas used to derive runup values are displayed in Chapter 2, and taken from Holman (1986) & Sallenger (2000). R_{HI} and R_{LO} values were recorded between scarp observations. In other words, each row contains the resulting scarp geometries (columns 4 & 5) based on the approximate runup values (columns 2 & 3) between scarp observations. Also, this table corresponds to figure 4.9, and should be used to aid in interpreting the figure.

5. Discussion

Chapter 5 will discuss the key results displayed in Chapter 4, and attempt to give semi-quantitative justifications for the patterns observed in an effort to better understand the morphological development of beach scarps. Figure 5.1 below displays a binary graphic intended to provide the reader with a final overview of when beach scarps actually existed at the Sand Engine in relation to the maximum water levels and average offshore wave power between each measurement period.

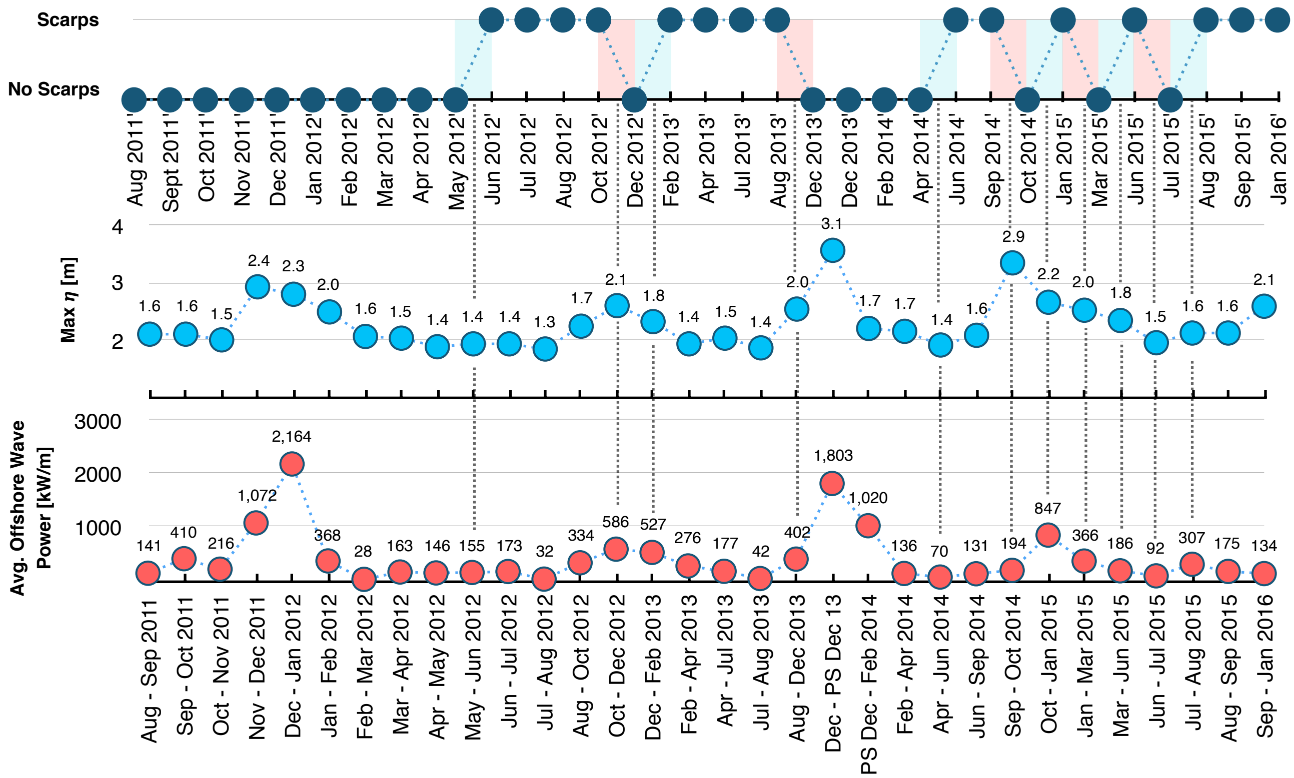

Figure 5.1 (Top) Binary plot demonstrating beach scarp existence at the Sand Engine between August 2011 & January 2016 (4.5 years). The blue and red shading denote periods of scarp creation and removal respectively. (Middle) Maximum water levels in meters NAP recorded in the Sceveningen Harbour between each measurement period. (Bottom) Average offshore wave power calculated using the average wave conditions recorded at the Europlatform between each measurement period. The domain of the middle & bottom plots are off-centered from the top plot, as these show the hydrodynamics recorded between each morphologic measurement. The black dotted lines are intended to provide the reader with a clear indication of the hydrodynamic values corresponding to scarp creation & removal.

5.1. Along- & Cross-Shore Development

Shoreline change is affected by a multitude of complex processes operating at different time and length scales (Larson & Kraus, 1995; Miller & Dean, 2004). Wave dominated cross- & long-shore transport, wave setup, and storm surge are the dominant processes influencing shoreline change on energetic coastlines at smaller time scales. Beach scarping appears to be relatively sensitive to the initial profile geometry and the concurrent hydrodynamic conditions, particularly wave climate and storm surge.

These cliff-like features were observed at the Sand Engine during 15 of the 33 measurement periods, and were most persistent between June 2012 and August 2013. There is a strong seasonal signal with 8 of 15 observations occurring during summer measurements. The northern hemisphere seasons are typically divided into three month intervals with summer being June 1st to August 31st and winter being December 1st to February 28th. The first two reset events, where persistent scarps were removed, were observed during the December 2012 & 2013 measurement periods (Northern Hemisphere Winter); furthermore, the maximum water levels were +2.1 and +2 m NAP, respectively (see figure 5.1). From section 4.3, it can be seen that scarping consistently occurs between elevations of +1.5 & +3 m NAP; meaning the still water level was slightly greater than or equal to the scarp toe elevation (S_{LO}) during these December periods. The resulting wave runup (R_{HI}) for these removal periods was 3.79 m and 3.99 m respectively, indicating the overtopping and/or inundation regime led to scarp destruction.

There were a total of 5 removal periods observed (figure 5.1 - red shading), of which 4 contained maximum water levels of at least +2 m NAP and 1 reaching a maximum of +1.5 m NAP. The first 4 are in line with the hypothesized framework in that the resulting runup values must exceed the scarp crest in order for the scarp to be removed. The final removal period occurred between June and July 2015 (Northern Hemisphere Summer), where scarp disappearance was observed along the 1403 m and 1440 m transects; however, after further examination, the steep sections in these profiles are not very pronounced. In other words, a scarp was identified through both methods, but the uncertainties in scarp identification may explain this outlier.

Summer-winter behavior of the profile may occur when a calm period is interrupted by a storm event. For instance, from figure 5.1, we can see that a storm occurred prior to the measurement periods of June 2014 & 2015 (Northern Hemisphere Summer), which resulted in beach scarp development. This tells us that not only are high energy events capable of destroying scarps, but also generating them. However, this also gives indication that there are critical thresholds in hydrodynamics which will yield different morphologic results. The average offshore wave power and max η [m] for each of these periods was calculated to be 70 and 186 kW/m & 1.4 and 1.8 m NAP, respectively.

Similar to that of Seymour et al. (2005), we can see that beach scarps result in an alongshore quasi-periodic variability. It was prevalent at the southern flank in the earlier months after construction was complete (June - August 2012), but favored the head and point beyond August 2013 (see figure 4.2). That being said, the periods of July and August 2013 seem to yield a rather uniform longshore distribution, with scarps extending nearly the entire perimeter of the peninsula. From the table provided in appendix

A, it can be seen that pronounced sandbars and nearshore banks at the Sand Engine existed concurrently with all instances of beach scarping, indicating the nearshore slopes and wave breaking are extremely important to the development of these features. Another interesting result observed in figure 4.3 was the variation in scarp height distribution with respect to the longshore direction. Originally, this was attributed to the measurement uncertainties mentioned in Chapter 3; however, it seems possible from examining the patterns that these undulations in scarp height were caused by sectional overtopping and/or slumping events. Should the runup exceed a section of the crest, this segment may appear different than the adjacent segment due to partial destruction. This could also be attributed to irregularities in wave height distribution and/or swash excursions (see figure 5.2 - right & left).

Figure 5.2 (Left) Aerial image of beach scarping at the Sand Engine from November 15th, 2015. Image from the Dutch Ministry of Infrastructure and the Environment. One should also notice the pronounced 3-D morphology (runnels and sand banks) in the intertidal zone insinuating strong alongshore tidal currents. (Right) Beach scarp at the head of the Sand Engine taken during the August 2013 measurements. Photo taken from Shore Monitoring (2013).

Section 4.3 analyzes a few representative transects at selected time periods in an attempt to better see how the profile changes and scarps develop along the perimeter of the Sand Engine. From the figures presented, it can be seen that beach scarps seem to develop as a result of the profile becoming more concave with respect to the incoming wave direction; the lower intertidal becomes more flat, while simultaneously steepening the higher section of the profile (see figure 4.4 - solid green line).

Once a scarp has fully developed, it remains persistent in time and space until the water levels and wave energy increase to a level where they can actually influence these features. This is due to the scarp crest being consistently located at approximately +3 m NAP (scarp toe 30 - 80 cm below crest), allowing it to be preserved if the runup levels do not reach the scarp base. Take, for example, the periods of July and August 2013 (Northern Hemisphere Summer); the maximum water levels were 1.5 & 1.4 m NAP respectively, with moderate wave conditions, allowing the scarp to maintain its structure.

To validate the beach scarp observations and hypothesized regime framework described in Chapter 2, approximate runup values were calculated along the 1100 m transect in section 4.3. The run-up (R_{HI}) and rundown (R_{LO}) values were calculated using maximum water levels and wave conditions between each measurement period, along with the cross-shore slope between +2 to -1 m NAP elevations. The regime framework proved valid 4 out of 5 times along this particular transect. The outlier being the August 2013 measurement period, which showed the scarp decreased in height by approximately 14 cm; however, this decrease in height was unexpected considering R_{HI} never reached the scarp toe, indicating the swash regime (2.29 m < 2.50 m). This may be attributed to the fact that these runup values are first-order approximations and do not take things like wave direction and refraction into account. Additionally, the decrease in height was due to a higher toe elevation insinuating some sort of deposition at the base due to slumping; this could have been caused by high wind speeds or drying of the sand.

The tidal range at the Sand engine is approximately 1.7 m with the majority of the scarp toe elevations occurring at approximately +2 m NAP. Also, figure 5.2 (left) displays strong 3-dimensional features in the intertidal zone insinuating the longshore tidal currents play a large role in the morphology of this region. Figure 5.1 reinforces this strong dependency on tidal elevations and nearshore wave energy. Another reason the longshore currents are suspected to play a large part in beach scarp development is due to similar scarp-like features appearing in the tidal lagoon (see Appendix F). The strong current velocities appear to erode the sand banks of the lagoon in a similar fashion resulting in steep morphologic features.

The following section will give a final overview of the significant findings displayed in this report and summarize the semi-validated regime framework. It will also go on to give suggestions for improving results and further research ideas in order to better understand this vaguely understood topic.

6. Conclusion

The ability to predict coastal morphology on medium to large time scales (years to decades) based on hydrodynamic conditions has significantly increased in recent years; however, our ability to predict beach erosion and transport rates above the still water level on smaller time scales is still lacking. This is partially due to measurement limitations and lack of sufficient datasets which show pre- & post-storm profile changes. In this study, a survey dataset taken at the Sand Engine mega-nourishment on the southwest coast of Holland was analyzed in an attempt to locate beach scarps and characterize their development.

The dataset consisted of 33 measurements spanning from August 2011 to January 2016 (4.5 years). The method used to identify the scarps was taken from Ruiz de Algria-Arzaburu et al. (2013), where the scarp crest and toe were identified through the local minimum and maximum of the second order derivative of the profile elevations respectively. However, manual transect analysis was also implemented in order to validate the automated results. Scarps of at least 30 cm in height were observed 15 out of the 33 morphologic measurement periods.

The subaerial cross-shore profile evolution was observed in an effort to gain insight on beach scarp initiation and recession processes. It begins with the lower part of the profile eroding as an early response to increasing energy levels causing the cross-shore surface to become more concave with respect to the incoming waves. This concave upward geometry is created through erosion of the lower intertidal resulting in the natural construction of a berm due to swash motions. As the concavity of the profile increases, the lower intertidal slope becomes more flat, while the upper profile slope steepens; thus, steepening to the point of developing into a so-called scarp. Although this profile steepening process is clearly observed, the actual physics behind the moment of initiation remains an ambiguous topic, requiring more instantaneous measurement details.

Beach scarps at the Sand Engine yield a strong seasonal signal which is to be expected, considering the majority of observations occurred during summer months when the wave climate was relatively moderate ($S_{HI} >> R_{HI}$). However, we also observed summer-winter profile behavior when a calm period was interrupted by a storm event. It was observed that these high energy events led to both the removal and creation of scarps at the Sand Engine, which means that not only are high energy events capable of destroying scarps, but also generating them. However, this also gives indication that there are critical thresholds in hydrodynamics which will yield different morphologic results.

Therefore, by considering how runup levels vary relative to scarp crest and toe elevations, a series of impact regimes were validated using the survey dataset taken at the Sand Engine. Table 6 demonstrates this regime framework and gives specific details on expected morphological change based on the results observed in this research paper.

Impact Level	Ranges	Regimes and Morphology Predictions
I	$R_{HI} < S_{LO}$	• Runup is confined to the lower foreshore of the beach and does not typically reach the base of the scarp; thus leaving it unaffected
II	$S_{HI} > R_{HI} > S_{LO}$	• Runup collides with the base of the beach scarp creating an undercutting effect which creates instabilities in the upper profile; this may lead to 'notching' or 'slumping' which will cause the scarp to recede landward, but stay in tact.
III	$R_{HI} > S_{HI} > R_{LO}$	• The runup levels are above the scarp crest during this regime allowing energetic waves to overtop the scarp crest. This may lead to the destruction of scarps, but not always. In some cases, it may lead to alongshore variability in scarp height and a net onshore transport of sand.
IV	$R_{LO} \geqq S_{HI}$	• The rundown levels are slightly larger than or equal to the scarp crest during this regime and the upper beach edge basically acts as the traditional surf zone. This led to the demise of scarps at the Sand Engine.

Table 6. Table describing validated regime changes after Sallenger (2000). (Impact level I.) The 'swash' regime occurs when the wave run-up is confined to the lower foreshore section of the existing beach; water levels are not high enough for the resulting run-up to influence the beach scarp too drastically. (Impact level II.) The 'collision' regime occurs when the resulting run-up becomes large enough to reach the base of the scarp; typically, the toe will be eroded away as the scarp is impacted by the uprising swash. (Impact level III.) The 'overtopping' regime begins once the runup levels exceed the scarp crest; the water level is slightly larger or equal to the scarp toe elevation allowing the scarp crest to be overtopped by the incoming uprush caused by energetic waves. (Impact level IV.) The 'inundation' regime occurs when the storm surge level surpasses the scarp crest elevation; in this scenario, the upper part of the profile is completely subaqueous and it generally leads to destruction os scarps.

The findings imply scarps follow an overall pattern of periodic variability at the Sand Engine depending on the original profile geometry, water levels (storm surge & tidal elevation), and wave runup events. Scarping consistently occurs between +3 & +1.5 m NAP elevations, with the average scarp height at the southern flank, head, and point being 0.85, 0.78 & 1.0 m respectively. Observations showed that already developed scarps were only affected when the maximum runup levels (R_{HI}) exceeded the scarp toe (S_{LO}); so, when (R_{HI}) $\geqq$ +1.5 m NAP approximately (collision regime, overtopping, and inundation regimes). The collision regime is responsible for the landward migration of the scarp crest (S_{HI}) without destroying the entire feature; the runup elevation is able to reach the scarp base inducing an undercutting effect which leads to slumping of the scarp face, but not necessarily to complete destruction. Furthermore, scarps were completely removed only upon entering the overtopping and/or inundation regimes. It appeared the swash regime had no effect on the scarps at all considering the geometric characteristics remained approximately constant between measurement periods, insinuating the water levels were not high enough for the resulting runup to reach the scarp base. Thus, storm surge and tidal elevations have a strong influence on scarp generation/degradation at the Sand Engine, by exposing a greater area of the coast to wave attack.

Recommendations

Beach scarp development is a common occurrence on newly nourished beaches around the world. That being said, they remain a poorly understood subject, particularly when it comes to initiation mechanisms. Presently, a general knowledge regarding their behavior in relation to the concurrent hydrodynamics has been demonstrated through representative scarps along the perimeter of the Sand Engine. However, there is much room for further research. The bullet points below contain recommendations for future research ideas pertaining to the current dataset used in this report:

- A Bayesian network relies on existing data to make decisions, while also accounting for uncertainty at the same time. These are typically used to unify several components of a complex system into one network. Limitations in Bayesian networks typically include those pertaining to the dataset; however, this Sand Engine dataset is rather complete with a large spread of measurements. Therefore, I recommend implementing all seemingly important parameters/controls that pertain to beach scarping into a Bayesian Network to see if it yields some level of predictability. In particular, runup would be a good output parameter to assess under which hydrodynamic conditions a scarp might occur.

- Utilize a cross-shore process-based numerical model, like Xbeach, to see if scarps can be predicted to some degree through runup simulations. In recent years, process-based numerical models have become more accurate with scientific research and have substantially aided in sediment transport predictions. As beach nourishment schemes increase in popularity, there is a need for better understanding of erosion rates pertaining to this scarping phenomenon. A model like Xbeach currently takes things such as slumping and avalanching of dunes into consideration, so it would be interesting to see how the model performs in relation to beach scarp prediction and development. Also, processes like refraction and diffraction can be considered through use of this model, which would give more accurate runup values.
    1. Start out with the 1-D surf-beat mode of Xbeach implementing a fine grid resolution (< 1 m)
    2. If no scarps appear, try 2-D mode
    3. If no scarps appear, try refining the grid resolution even more

- Conduct a laboratory test similar to that of Payo et al. (2008), where a berm was constructed in a multi-directional wave basin, and water levels were raised in intervals to see how the profile responded. I also recommend the construction of a scarp (rather than just a berm) in which the experimenter would have control over all structural components such as grain size, compaction, geometry, etc. This will aid in providing more focus on how these features respond to certain hydrodynamic conditions without the structural uncertainties. This could be used to validate the regime change results examined in this report.

- Although aeolian transport seems to only effect scarps in the long term, perhaps this could be confirmed through the application of an aeolian transport model in order to more accurately estimate erosion rates.

- Interestingly enough, steep slopes resembling scarps have also been observed along the lagoon banks at the Sand Engine (see Appendix F). This insinuates that the longshore tidal currents may have some influence on scarp development. It could be interesting to examine the scarping process from a riverine flow standpoint to confirm this suspicion.

- Intertidal sand bank & sandbar locations appear important to scarp development, considering they appeared in the seaward direction of almost every scarp examined in this report (see Appendix A). It may be interesting to conduct further analysis on the specifics of bar existence & migration at the Sand Engine to see if this relation can be quantified.

- More instantaneous measurements should be conducted (e.g. pre- & post-storm measurements), considering the initiation of a beach scarp occurs at a smaller time scale. Daily contour maps of the beach could be created using a GPS-based surveying system that, coupled with video imaging of the beach may reveal details of scarp development.

- Finally, the structural components of the beach appear highly influential to beach scarping. In other words, this phenomenon may be correlated to sediment sizes, compaction, cohesiveness, etc. Better understanding of the stratigraphy and shell patterns observed in the scarp face at the Sand Engine may provide further insight to these occurrences (see Appendix F). Sherman & Nordstrom (1985) actually mention something called beach freezing, insinuating that the sand properties change due to decreasing temperature. Structural components such as this could potentially be implemented in the aforementioned Bayesian Network.

References

Anfuso, G., Benavente, J., & Gracia, F. J. (2001). Morphodynamic responses of nourished beaches in SW Spain. *Journal of Coastal Conservation*, *7*(1), 71-80.

Battjes, J.A., 1998. Surf-zone dynamics. Annual Review of Fluid Mechanics, 20(1), pp.257–291.

Bonte, Y. & Levoy, F., 2015. Field experiments of beach scarp erosion during oblique wave, stormy conditions (Normandy, France). Geomorphology, 236, pp.132–147.

Bosboom, J. & Stive, M.J.F., 2013. Coastal Dynamics I,

Carter, J., 1988. Digital Representations of Topographic Surfaces Carter J R 1988. Photogrammetric Engineering and Remote Sensing,, 54(11), pp.1577–1580.

de Alegria-Arzaburu, A. R., Mariño-Tapia, I., Silva, R., & Pedrozo-Acuña, A. (2013). Post-nourishment beach scarp morphodynamics. *Journal of Coastal Research*, *1*(65), 576.

de Schipper, M.A. et al., 2016. Initial spreading of a mega feeder nourishment: Observations of the Sand Engine pilot project. Coastal Engineering, 111, pp.23–38.

Dean, R. G. (1991). Equilibrium beach profiles: characteristics and applications. *Journal of coastal research*, 53-84.

Dean, R.G. & Dalrymple, R.A., 2002. Coastal Processes with Engineering Applications, Available at: http://www.cambridge.org.

Elko, N.A., Holman, R.A., Gelfenbaum, G., 2005. Quantifying the rapid evolution of a nourishment project with video imagery. *Journal of Coastal Research* 21(4).

Erikson, L.H., Larson, M. & Hanson, H., 2007. Laboratory investigation of beach scarp and dune recession due to notching and subsequent failure. Marine Geology, 245(1-4), pp.1–19.

Holthuijsen, L.H., 2007. Description of ocean waves. In Waves in Oceanic and Coastal Waters. pp. 24–55. Available at: http://ebooks.cambridge.org/ref/id/CBO9780511618536\nhttp://ebooks.cambridge.org/ref/id/CBO9780511618536A017.

Iribarren, C.R. & Nogales, C.M., 1949. Protection des ports, Available at: http://cedb.asce.org/cgi/WWWdisplay.cgi?9401349\nhttp://repository.tudelft.nl/view/hydro/uuid:7ab718ff-a74d-4141-8c3f-413044c751c4/.

Jackson, N.L. et al., 2010. Effects of nourishment on the form and function of an estuarine beach. Ecological Engineering, 36(12), pp.1709–1718.

Nishi, R., Sato, M., & Wang, H. (1995). Field Observation and Numerical Simulation of Beach and Dune Scarps.

Payo, A., Kobayashi, N., Munoz-Perez, J., & Yamada, F. (2008). Scarping predictability of sandy beaches in a multidirectional wave basin. *Ciencias Marinas*, *34*(1), 45-54.

Roelvink, D. & Reniers, A., 2012. A guide to modeling coastal morphology, Available at: http://www.vliz.be/imis/imis.php?module=ref&refid=212305.

Roelvink, D. et al., 2009. Modelling storm impacts on beaches, dunes and barrier islands. Coastal Engineering, 56(11-12), pp.1133–1152.

Sallenger, A.H., 2000. Storm Impact Scale for Barrier Islands. Journal of Coastal Research, 16(3), pp. 890–895.

Schwartz et al., 2005. Encyclopedia of Coastal Science, Available at: http://www.springer.com/gp/book/9781402019036.

Schwartz et al., 2005. Encyclopedia of Coastal Science, Available at: http://www.springer.com/gp/book/9781402019036.

Seymour, R. et al., 2005. Rapid erosion of a small southern California beach fill. Coastal Engineering, 52(2), pp.151–158.

Sherman, D. J., & Nordstrom, K. F. (1985). Beach scarps. *Zeitschrift Fur Geomorphologie*, *29*(2), 139-152.

Short, A.D. & Hesp, P.A., 1982. Wave, beach and dune interactions in southeastern Australia. Marine Geology, 48(3-4), pp.259–284.

Sorensen, R.M., 2006. Basic Coastal Engineering Basic Coastal, Available at: http://books.google.com/

Stive, M.J.F. et al., 2002. Variability of shore and shoreline evolution. Coastal Engineering, 47(2), pp. 211–235.

Wright, L.D. & Thom, B.G., 1977. Coastal depositional landforms: a morphodynamic approach. Progress in Physical Geography, 1(3), pp.412–459.

Wright, L. D. (1980). Beach cut in relation to surf zone morphodynamics. *Coastal Engineering Proceedings*, *1*(17).

Appendix A - Morphology Descriptions & Gridded Bathymetry

The table below gives a brief synopsis of the relative morphology measurements described by Shore Monitoring (2013) at each survey period for the first year and a half; this is intended to give the reader a general sense of the changing morphology at the Sand Engine with respect to developing cliffs, particularly along the perimeter where beach scarping is of interest.

No.	Survey Period	Time Lapse [days]	Relevant Morphology
1	**August 2011'**	-	- A narrow subtidal sandbank was observed all along the perimeter of the Sand Engine (Southern Flank, Head, Point) - A spit developed at the end of the point
2	**September 2011'**	30	- The subtidal sandbank along the perimeter of the Sand Engine (Southern Flank, Head, Point) still remains and is fairly uniform - Another sand bank has developed extending from the intertidal beach at Ter Heijde to the Southern Flank - The spit at the point is larger
3	**October 2011'**	41	- The subtidal sand bank along the perimeter is now broken in various places and is no longer continuous; - The sand bank also is positioned further from the Sand Engine than before between the point and spit only, which is partly due to erosion at the head and point - The sand bank at the head of the Sand Engine has been divided into three large sandbanks with broad rips in between - The sandbank extending from the intertidal beach at Ter Heijde along the southern flank is less prominently observed - The runnel between the sandbar and the Sand Engine has become deeper; runnel pits can be observed in the intertidal zone along the perimeter of the Sand Engine - The spit has widened and has extended further toward the beach at Kijkduin
4	**November 2011'**	28	- Large and pronounced sandbanks are observed all along the perimeter of the Sand Engine - Three large, pronounced sand banks exist at the head of the Sand Engine and have formed cusp-like features - The sand bank at the point is still unbroken in the longshore direction - The spit has become larger and wider, extending further north & towards the beach at Kijkduin - The majority of the intertidal areas at the Sand Engine during this period were smooth; Only at the point and the beach at Kijkduin are tidal pits observed

5	**December 2011'**	45	- Largest change in morphology observed thus far - The intertidal area along the perimeter of the Sand Engine has become flatter and wider in general - The area between the head and the spit has especially changed in that the spit has almost attached itself to the beach at Kijkduin; therefore, the shoreline at low tide has more of a gaussian shape - The three pronounced sand banks at the head have developed differently; southernmost bank has become wider; middle has become smaller and located further from the Sand Engine; the northernmost bank has become wider and moved closer to the Sand Engine - The sandbar along the point and spit shifted in the direction of kijkduin - The sandbar is higher and wider than previously observed
6	**January 2012'**	18	- The separate sandbanks are not very pronounced anymore as they have almost merged together again along the perimeter - There are two broad banks at the head and point, that are attached to the Sand Engine beneath the low water mark - the spit has continued to fill in and get wider - **small scarps (< 30 cm) are observed along the head and point** - considerable erosion along the entire perimeter
7	**February 2012'**	42	- Cusp shaped coastline at the head is becoming more pronounced with broad rips between them - the two broad sandbanks at the head and point are still connected to the intertidal - The sandbar along the southern flank has become wider and more alongshore uniform - **small scarps (< 30 cm) have developed along the head and point around the +2 m NAP contour**
8	**March 2012'**	24	- The elevation of the sandbank at the point has increased - the bottom positions of all intertidal sandbanks on the southern side is higher than previous measurements - There are several runnels and runnels spanning the entire lower intertidal sandbar
9	**April 2012'**	36	- The elevation of the sandbank at the point has increased; also, this sandbank nearly extended to the intertidal beach at Kijkduin - The sandbar at the head became larger and migrated further onshore - The runnels between the sandbar and Sand Engine at the point have deepened - The shoreline behind the sandbars seem to exhibit cusp-like features - **Small scarps are observed from the point to the beginning of the southern flank**

10	**May 2012'**	26	- the sandbanks at the head and point are well defined and connected to the intertidal region for the most part - **scarps were observed at the head and point in the order of 0.5 m** - the intertidal runnels on the south side of the Sand Engine are pronounced
11	**June 2012'**	24	- the sandbank along the southern flank to the head is fairly uniform and continuous - the sandbanks along the northern side of the Sand Engine are more irregular in shape and bottom position (i.e. not alongshore uniform); the position of the sandbank at the point is also higher than previous measurements with a deep runnel on the shoreward side; a small, narrow sandbar is beginning to develop on the seaward side of northern sandbank - **scarps were observed at the point in the order of 0.5 m; scarps were observed along the head and southern flank in the order of 1.5 m**
12	**July 2012'**	34	- The sandbanks at the head and point have moved towards the spit; also these features have been moved closer to the Sand Engine - Large gradients in bed elevations at the head and point have been observed - **The scarp at the point is adjacent to the high water line at quiet conditions**
13	**August 2012'**	27	- The intertidal sand banks at the head have increased in elevation and extended further towards the sea - Three large subtidal sandbanks have developed at the point; the intertidal in this region has increased in elevation and the resulting runnel has narrowed - **Prominent scarps were observed along the perimeter from the southern flank to the point**
14	**October 2012'**	46	- The three intertidal sandbanks at the point have become larger and more pronounced; they have also migrated further northwards - A fourth sand bank is now observed at the end of the point closer to the spit - Further seaward from these four sandbanks at the point, is a small narrow sandbar - **The scarps are still present on the landward side of the intertidal sandbanks along the perimeter**
15	**December 2012'**	68	- A dual sandbank system has again developed on the southern side of the Sand Engine near Ter Heijde (This was also observed during the winter of 2011, but disappeared during the summer) - The sand bar along the southern flank is relatively uniform - The sandbar on the northern side of the head appears further seaward - Scarps at the southern flank have disappeared

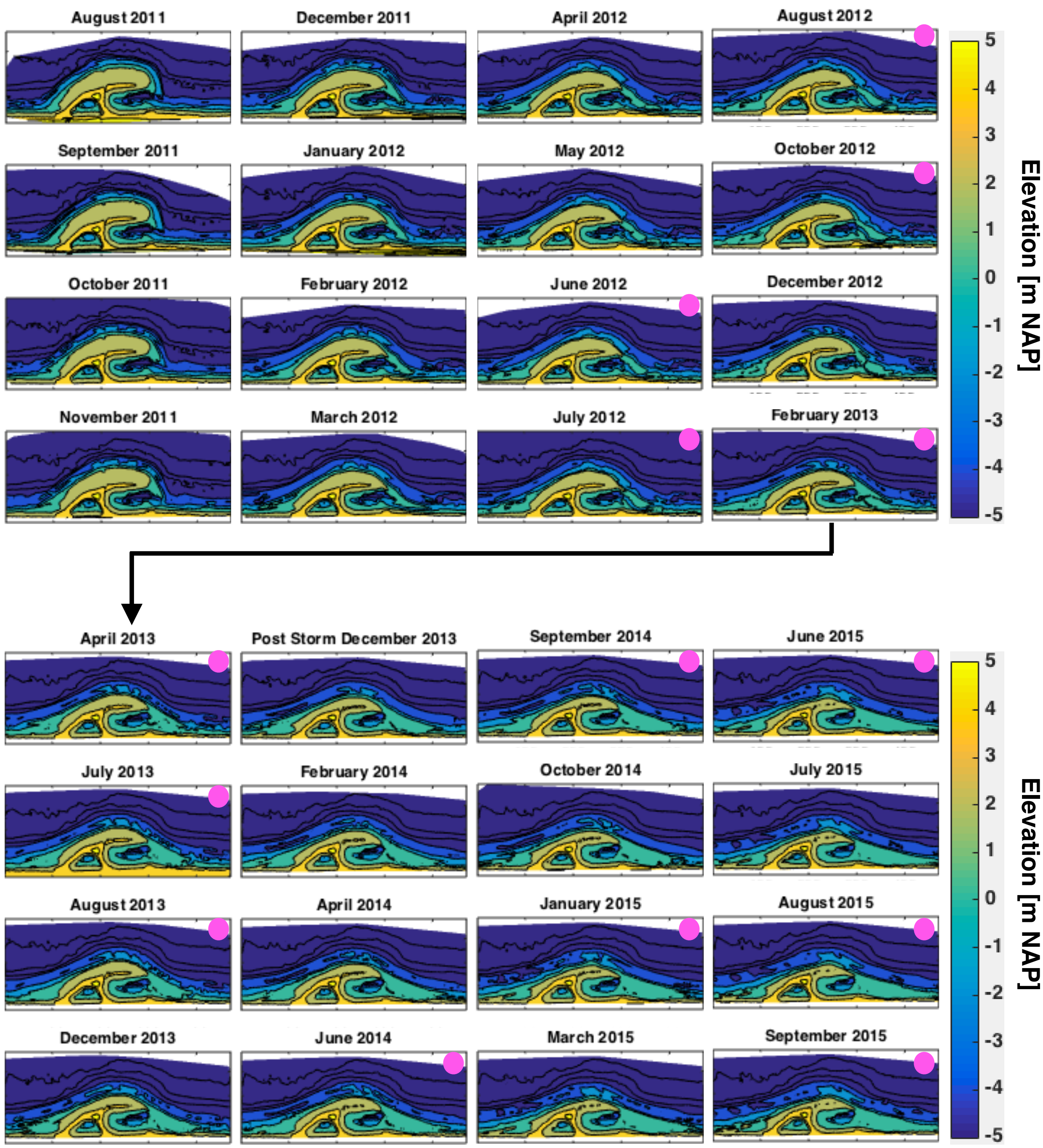

Figure A. Bathymetric plots of the Sand Engine spanning from August 2011 to September 2015. Magenta dots represent the periods where scarps were present along the perimeter. The reader should observe the pronounced sand bank formations along the edge of the peninsula.

Appendix B - Scarp Database

Survey Period	Manual Identification Database
	Alongshore Transect Position of Beach Scarps at the Sand Engine [m]
Aug 2011	-
Sep 2011	-
Oct 2011	-
Nov 2011	-
Dec 2011	-
Jan 2012	-
Feb 2012	-
Mar 2012	-
Apr 2012	-
May 2012	-
Jun 2012	550, 592, 632, 672, 765, 796, 828, 864, 902
Jul 2012	511, 552, 594, 612, 644, 674, 715, 831, 873, 1244, 1285, 1325, 1552, 1578, 1623
Aug 2012	507, 548, 588, 630, 671, 718, 763, 824,1188, 1236, 1263, 1580, 1621
Oct 2012	510, 552, 591, 632, 675
Dec 2012	-
Feb 2013	910, 949, 984
Apr 2013	589, 630, 671, 717, 765, 1018, 1057, 1098, 1140, 1162, 1233, 1276, 1324, 1403, 1440, 1478, 1519, 1550
Jul 2013	429, 474, 551, 591, 635, 756, 797, 822, 865, 900, 939, 977, 1018, 1062, 1099, 1163, 1186, 1229, 1280, 1331, 1364, 1404, 1449, 1483, 1548, 1578
Aug 2013	407, 431, 471, 512, 584, 718, 765, 792, 826, 948, 981, 1067, 1099, 1234, 1280, 1322, 1355, 1403
Dec 2013	-
PS Dec 13	-
Feb 2014	-
Apr 2014	-
Jun 2014	1165, 1189, 1240, 1280, 1321
Sep 2014	798, 862, 907, 942, 984, 1029, 1062, 1105, 1142, 1163, 1192, 1234, 1280, 1322, 1355, 1403
Oct 2014	-
Jan 2015	1190, 1205
Mar 2015	-
Jun 2015	1403, 1440
Jul 2015	-
Aug 2015	675, 725, 768, 798, 825, 1403
Sep 2015	720, 770, 795, 827, 1400, 1443
Jan 2016	720, 765, 795, 1400, 1443

Table B.1. This table demonstrates the located scarps with respect to alongshore position using the manual identification method described in Chapter 3.

Survey Period	Automated Tool Database
	Alongshore Transect Position of Beach Scarps at the Sand Engine [m]
Aug 2011	-
Sep 2011	-
Oct 2011	-
Nov 2011	-
Dec 2011	-
Jan 2012	-
Feb 2012	-
Mar 2012	-
Apr 2012	-
May 2012	820
Jun 2012	505, 540, 575, 645, 785, 820, 855, 1555, 1590
Jul 2012	540, 610, 645, 680, 890, 1590
Aug 2012	540, 575, 680, 715, 1205, 1240, 1590
Oct 2012	505, 540, 575, 610, 680
Dec 2012	-
Feb 2013	995, 1065, 1100, 1310
Apr 2013	715, 1100, 1240, 1275, 1310, 1450, 1485, 1520, 1555
Jul 2013	400, 435, 470, 505, 575, 610, 645, 680, 715, 750, 785, 855, 890, 925, 960, 995, 1030, 1065, 1100, 1135, 1170, 1205, 1240, 1275, 1310, 1345, 1380, 1415, 1450, 1485, 1520, 1555, 1590
Aug 2013	435, 470, 575, 610, 645, 750, 785, 925, 960, 995, 1065, 1100, 1135, 1170, 1205, 1240, 1275, 1310, 1345, 1380, 1415, 1450, 1485, 1520, 1555, 1590
Dec 2013	-
PS Dec 13	-
Feb 2014	-
Apr 2014	-
Jun 2014	-
Sep 2014	785, 820, 960, 995, 1030, 1065, 1100, 1135, 1205, 1240, 1275, 1310, 1345, 1380, 1415
Oct 2014	-
Jan 2015	-
Mar 2015	785, 820
Jun 2015	715, 820, 1415
Jul 2015	785
Aug 2015	-
Sep 2015	785, 820, 855, 1415
Jan 2016	750, 785, 855

Table B.2. This table demonstrates the located scarps with respect to alongshore position using the automated identification method described in Chapter 3.

Appendix C - Runup & Average Offshore Wave Power

Measurement Period	Max $H_{s,0}$ [m]	Max $T_{m02,0}$ [s]	Max η [m]	Slope Head [+2 : -1 m NAP]	L_0 [m]	(ξ) Iribarren No.	$R_{2\%}$ [m]	$S_{2\%}$ [m]	S_{HIGH} [m]	S_{LOW} [m]	R_{HIGH} [m]	R_{LOW} [m]
Aug - Sep 2011	3.18	6.5	1.60	0.030	65.9	0.14	1.00	0.56	-	-	2.60	2.04
Sep - Oct 2011	4.13	6.7	1.60	0.039	70.0	0.16	1.38	0.81	-	-	2.98	2.16
Oct - Nov 2011	3.16	6.3	1.50	0.042	61.9	0.19	1.12	0.69	-	-	2.62	1.93
Nov - Dec 2011	**5.59**	**7.5**	**2.43**	**0.029**	**87.8**	**0.11**	**1.65**	**0.88**	**-**	**-**	**4.08**	**3.20**
Dec - Jan 2012	5.13	7.1	2.30	0.030	78.6	0.12	1.53	0.82	-	-	3.83	3.01
Jan - Feb 2012	3.93	6.4	1.99	0.025	63.9	0.10	1.11	0.57	-	-	3.10	2.53
Feb - Mar 2012	2.63	5.9	1.56	0.025	54.3	0.11	0.77	0.41	-	-	2.33	1.92
Mar - Apr 2012	3.25	6.7	1.53	0.029	70.0	0.13	1.01	0.57	-	-	2.54	1.98
Apr - May 2012	2.49	6.1	1.38	0.027	58.0	0.13	0.77	0.43	-	-	2.15	1.72
May - Jun 2012	4.04	6.7	1.43	0.026	70.0	0.11	1.17	0.61	-	-	2.60	1.99
Jun - Jul 2012	3.75	6.2	1.43	0.029	60.0	0.12	1.11	0.59	-	-	2.54	1.95
Jul - Aug 2012	1.78	5.9	1.34	0.035	54.3	0.19	0.64	0.40	-	-	1.98	1.58
Aug - Oct 2012	4.80	6.9	1.74	0.037	74.3	0.15	1.54	0.88	-	-	3.28	2.40
Oct - Dec 2012	4.63	7.3	2.10	0.047	83.1	0.20	1.69	1.06	-	-	3.79	2.73
Dec - Feb 2013	3.70	6.6	1.82	0.052	68.0	0.22	1.42	0.92	3.08	2.24	3.24	2.32
Feb - Apr 2013	3.34	6.4	1.43	0.056	63.9	0.24	1.35	0.90	2.85	1.76	2.78	1.88
Apr - Jul 2013	3.10	6.5	1.53	0.048	65.9	0.22	1.19	0.77	3.05	2.50	2.72	1.95
Jul - Aug 2013	2.23	6.0	1.36	0.052	56.2	0.26	0.93	0.63	3.05	2.64	2.29	1.66
Aug - Dec 2013	**5.33**	**7.5**	**2.04**	**0.049**	**87.8**	**0.20**	**1.95**	**1.22**	**-**	**-**	**3.99**	**2.77**
Dec - PS Dec 13	**4.89**	**7.2**	**3.07**	**0.034**	**80.9**	**0.14**	**1.54**	**0.87**	**-**	**-**	**4.61**	**3.74**
PS Dec - Feb 2014	**4.69**	**7.1**	**1.70**	**0.035**	**78.6**	**0.14**	**1.50**	**0.85**	**-**	**-**	**3.20**	**2.34**
Feb - Apr 2014	2.77	6.2	1.65	0.050	60.0	0.23	1.09	0.71	-	-	2.74	2.02
Apr - Jun 2014	**3.59**	**6.4**	**1.41**	**0.060**	**63.9**	**0.25**	**1.47**	**0.99**	**-**	**-**	**2.88**	**1.89**
Jun - Sep 2014	4.24	6.8	1.58	0.051	72.1	0.21	1.59	1.01	3.04	1.7	3.17	2.16
Sep - Oct 2014	**5.38**	**7.2**	**2.85**	**0.036**	**80.9**	**0.14**	**1.70**	**0.96**	**-**	**-**	**4.55**	**3.59**
Oct - Jan 2015	4.61	6.8	2.16	0.024	72.1	0.09	1.29	0.65	-	-	3.45	2.80
Jan - Mar 2015	4.39	6.8	2.02	0.032	72.1	0.13	1.35	0.75	-	-	3.37	2.62
Mar - Jun 2015	**4.26**	**6.7**	**1.84**	**0.023**	**70.0**	**0.09**	**1.18**	**0.59**	**-**	**-**	**3.02**	**2.43**
Jun - Jul 2015	2.62	6.5	1.45	0.030	65.9	0.15	0.85	0.49	-	-	2.30	1.81
Jul - Aug 2015	**4.33**	**6.7**	**1.62**	**0.030**	**70.0**	**0.12**	**1.30**	**0.70**	**-**	**-**	**2.92**	**2.22**
Aug - Sep 2015	3.58	6.5	1.62	0.041	65.9	0.18	1.24	0.75	-	-	2.86	2.11
Sep - Jan 2016	2.96	5.6	2.09	0.025	48.9	0.10	0.84	0.43	-	-	2.93	2.50

Table C.1 Scarp crest (S_{HI}) and toe (S_{LO}) elevations along the 1100 m transect versus high (R_{HI}) and low (R_{LO}) runup approximations. Formulas used to derive runup values are displayed in Chapter 2, and taken from Holman (1986) & Sallenger (2000). R_{HI} and R_{LO} values were recorded using the hydrodynamics between scarp observations. Also, this table corresponds to figure 4.9, and should be used to aid in interpreting the figure. Red text denotes periods where storms were recorded.

Measurement Period	Avg $H_{s,0}$ [m]	Avg $T_{m02,0}$ [s]	L_0 [m]	rho*g*n	c [m/s]	Avg Po [kW/m]
Aug - Sep 2011	1.04	4.08	1.69	314.53	0.41	140.86
Sep - Oct 2011	1.38	4.34	2.97	314.53	0.68	409.84
Oct - Nov 2011	1.15	3.98	2.06	314.53	0.52	215.90
Nov - Dec 2011	**1.79**	**4.66**	**4.98**	**314.53**	**1.07**	**1072.04**
Dec - Jan 2012	2.19	5.21	7.48	314.53	1.44	2163.65
Jan - Feb 2012	1.34	4.32	2.81	314.53	0.65	368.31
Feb - Mar 2012	0.69	4.10	0.75	314.53	0.18	27.58
Mar - Apr 2012	1.11	4.53	1.92	314.53	0.42	163.36
Apr - May 2012	1.07	4.42	1.79	314.53	0.41	146.22
May - Jun 2012	1.09	4.41	1.84	314.53	0.42	154.69
Jun - Jul 2012	1.11	4.30	1.92	314.53	0.45	172.60
Jul - Aug 2012	0.70	3.78	0.77	314.53	0.20	31.72
Aug - Oct 2012	1.31	4.37	2.69	314.53	0.62	333.94
Oct - Dec 2012	1.52	4.47	3.60	314.53	0.81	586.34
Dec - Feb 2013	1.47	4.39	3.38	314.53	0.77	526.54
Feb - Apr 2013	1.25	4.37	2.45	314.53	0.56	275.82
Apr - Jul 2013	1.11	4.26	1.93	314.53	0.45	176.75
Jul - Aug 2013	0.76	3.94	0.91	314.53	0.23	42.45
Aug - Dec 2013	**1.38**	**4.36**	**2.95**	**314.53**	**0.68**	**402.08**
Dec - PS Dec 13	**2.10**	**5.24**	**6.85**	**314.53**	**1.31**	**1802.80**
PS Dec - Feb 2014	**1.76**	**4.57**	**4.81**	**314.53**	**1.05**	**1020.21**
Feb - Apr 2014	1.04	4.16	1.68	314.53	0.40	136.37
Apr - Jun 2014	**0.88**	**4.27**	**1.22**	**314.53**	**0.28**	**69.81**
Jun - Sep 2014	1.03	4.14	1.64	314.53	0.40	130.95
Sep - Oct 2014	**1.14**	**4.30**	**2.03**	**314.53**	**0.47**	**194.13**
Oct - Jan 2015	1.68	4.65	4.42	314.53	0.95	847.14
Jan - Mar 2015	1.35	4.39	2.82	314.53	0.64	366.11
Mar - Jun 2015	**1.13**	**4.31**	**1.99**	**314.53**	**0.46**	**185.79**
Jun - Jul 2015	0.94	4.12	1.37	314.53	0.33	92.17
Jul - Aug 2015	**1.29**	**4.45**	**2.60**	**314.53**	**0.58**	**306.97**
Aug - Sep 2015	1.10	4.13	1.89	314.53	0.46	174.58
Sep - Jan 2016	1.02	3.96	1.62	314.53	0.41	134.02

Table C.2 Average offshore wave power (column 7) was calculated using [$P_0 = 1/16\rho g H^2_S c_g$]. The table in this section shows the values used in the calculations including daily averaged significant wave heights and corresponding wave periods (columns 2 & 3). Column 4 shows the wave length calculated using linear wave theory. The density of seawater was taken as 1025 kg/m^3 and 'n' was assumed to be 0.5 considering we are looking at the conditions in deep water. The gravitational acceleration is denoted by 'g' and was taken as 9.81 m/s^2. Red text denotes periods where a storm was recorded.

Appendix D - Scarp Recession

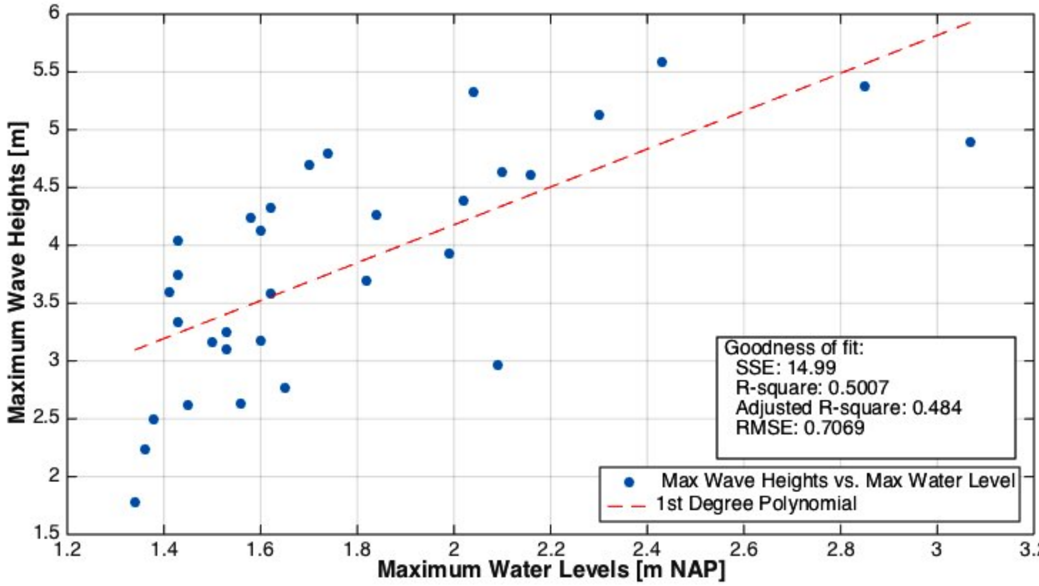

Figure D.1. Scatter plot intended to show correlation between maximum water levels and maximum wave heights at the Sand Engine. $R^2 = 0.50$.

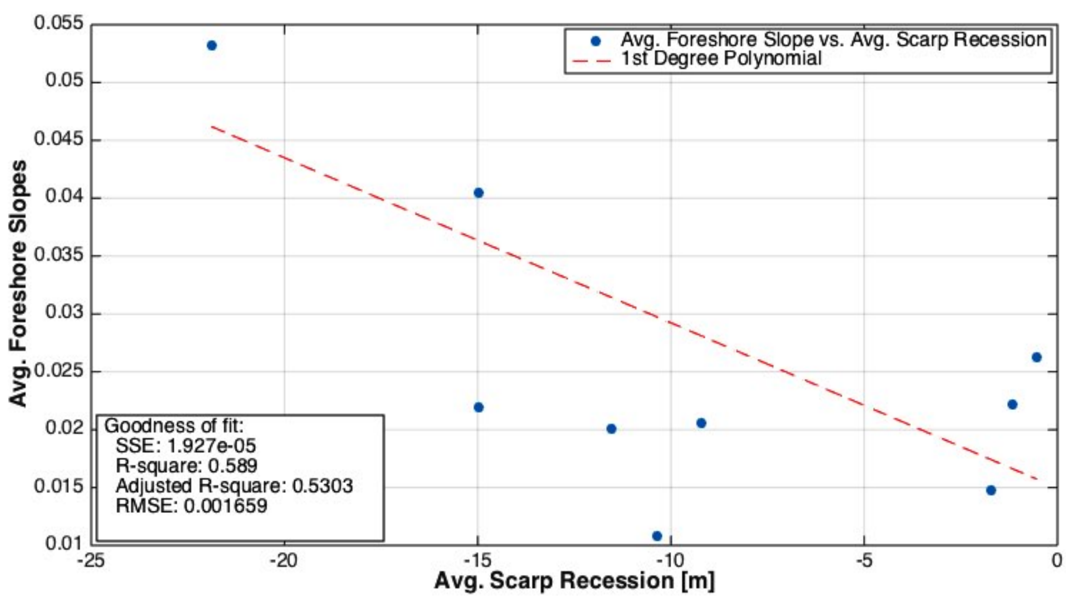

Figure D.2. Scatter plot intended to show correlation between average foreshore slope and average scarp recession in meters. $R^2 = 0.589$.

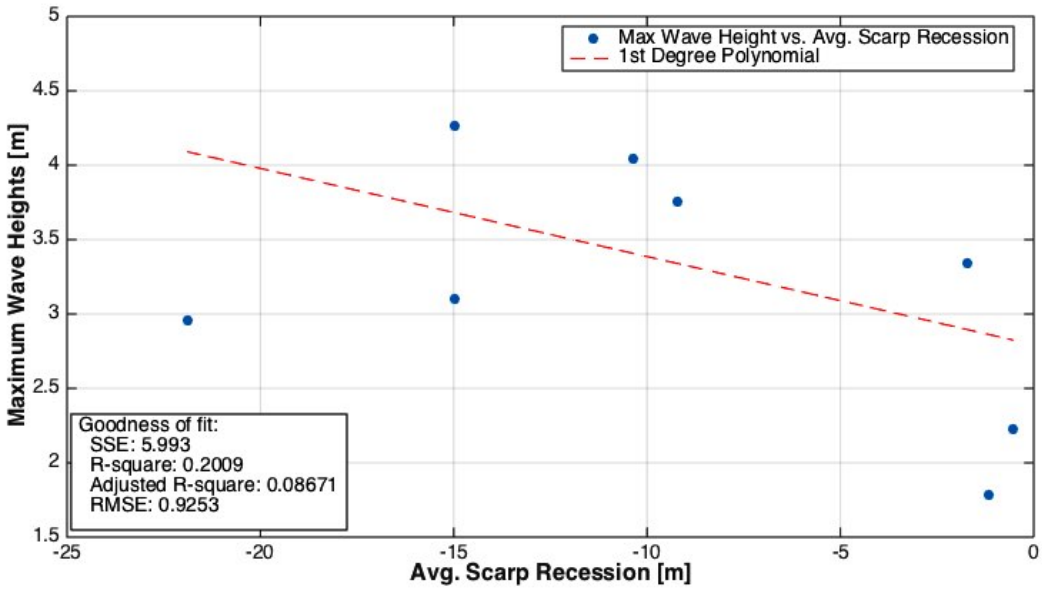

Figure D.3. Scatter plot showing correlation between maximum wave heights recorded at the Europlatform and average scarp recession in meters. $R^2 = 0.20$.

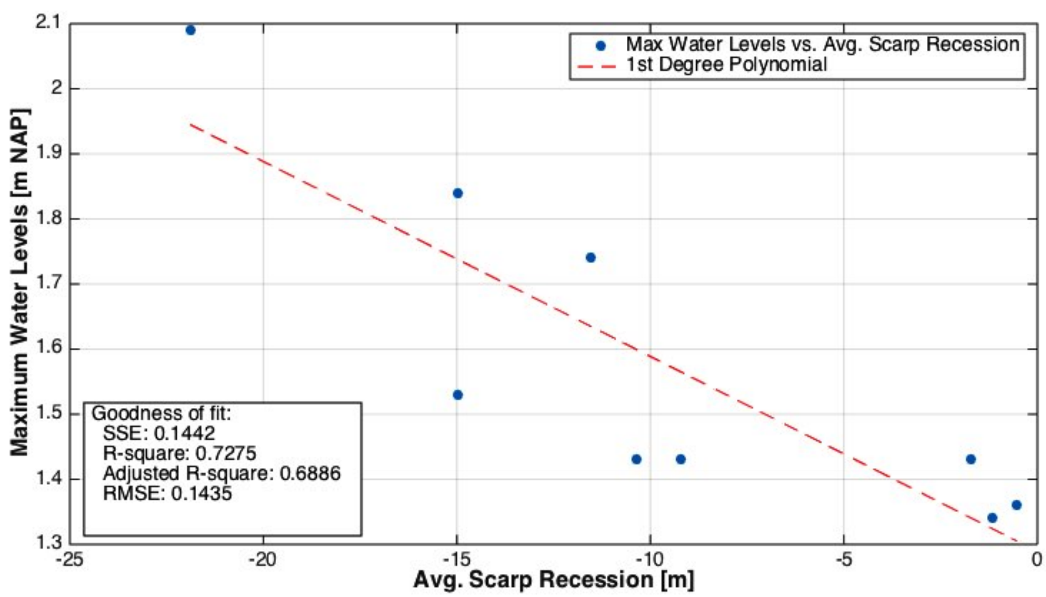

Figure D.4. Scatter plot showing correlation between maximum water levels recorded in the Scheveningen Harbour and average scarp recession in meters. $R^2 = 0.73$. This plot reinforces the main conclusion of this paper in that the water levels and resulting runup magnitudes are most influential.

Appendix E - Automated Matlab Script

```
%% Load data
load('AllZMbeachsurveys.mat');

yCrest = cell(numel(ZMsurvey),35);
yToe = cell(numel(ZMsurvey),35);
slopeScarp = cell(numel(ZMsurvey),35);
ScarpHeight = cell(numel(ZMsurvey),35);
foreshoreslope = cell(numel(ZMsurvey),35);
date = zeros(numel(ZMsurvey),1);

runs = 1:33;                                    % 1: numel(ZMsurvey)
% ----------------------------
for surveynr = runs(1):runs(end)
   [yCrest1,yToe1,slopeScarp1,ScarpHeight1,foreshoreslope1] = JDD_scarpFinder(surveynr);

   yCrest(surveynr,:) = yCrest1;
   yToe(surveynr,:) = yToe1;
   slopeScarp(surveynr,:) = slopeScarp1;
   ScarpHeight(surveynr,:) = ScarpHeight1;
   foreshoreslope(surveynr,:) = foreshoreslope1;
   surveynr
   date(surveynr)=ZMsurvey(surveynr,1).matlabdate;
end

% Gets rid of empty cell rows
HTmat = cell2mat(ScarpHeight);
SSmat = cell2mat(slopeScarp);
yCrestMat = cell2mat(yCrest);
yToemat = cell2mat(yToe);
foreshoreslopemat = cell2mat(foreshoreslope);
```

```
function [yCrest,yToe,slopeScarp,ScarpHeight,foreshoreslope] = JDD_scarpFinder(surveynr)
% ------------------------------------------------------------------
% STANDALONE INPUT
% ------------------------------------------------------------------
if nargin < 1
   surveynr = 20;                                   % the survey you are interested in
end
% ------------------------------------------------------------------
% MANUAL INPUTS
% ------------------------------------------------------------------
% Load XYZ data
load('AllZMbeachsurveys.mat');
xp=ZMsurvey(surveynr).paths.path_rot(:,1); % X
yp=ZMsurvey(surveynr).paths.path_rot(:,2); % Y
zp=ZMsurvey(surveynr).paths.path_rot(:,3); % Z

ngridpoints = 500;                                  % number of sections along the transect line

% Transect Locations
xes = 400:35:400+35*34; xes = xes';
yes1 = ones(length(xes),1).*575;
yes2 = ones(length(xes),1).*1150;
transec = [xes,yes1,xes,yes2];                      % x1,y1,x2,y2
slopeBuffer = 15;                         % max distance away from steepest part to look for toe

% ------------------------------------------------------------------
ntransects = 35;                             % number of transects

%% Define grid point arrays for each transect
xvals = zeros(ntransects,ngridpoints);          % each row is a transect
yvals = zeros(ntransects,ngridpoints);          % each row is a transect
zvals = cell(1,ntransects);                     % one row, each cell is a z-matrix

% Interpolate the data to the grid points for each transect
for j3=1:ntransects

   % Define x and y grid points for grid generation
   xvals(j3,:) = linspace(transec(j3,1),transec(j3,3),ngridpoints);
   yvals(j3,:) = linspace(transec(j3,2),transec(j3,4),ngridpoints);

   % Input into the griddata function
   xcor = xvals(j3,:);
   ycor = yvals(j3,:);

   % Note on griddata: xcor and ycor must be same dimensions
   % to have output that makes sense. For example, if you have a 2D
   % matrix instead of a transect, see
   % http://nl.mathworks.com/help/matlab/ref/griddata.html
```

```
    % Suppress warning that comes from griddata
    wid = 'MATLAB:scatteredInterpolant:DupPtsAvValuesWarnId';
    warning('off',wid);

    % Keep this as a cell, in case of 2D matrix output
    zvals{j3} = griddata(xp,yp,zp,xcor,ycor);
    warning('on',wid);
end

%% subaerial (above 0m NAP)
zp_subaerial = cell(1,ntransects); % pre-allocate
yp_subaerial = cell(1,ntransects); % pre-allocate

for j5=1:ntransects
%Cell arrays used here, because each transect could have a different number of points
    zp_subaerial{j5}= zvals{j5}(zvals{j5}>0);
    yp_subaerial{j5}= yvals(j5,zvals{j5}>0);
end

%% 1st and 2nd Derivatives
DZ = cell(1,ntransects); DZ2 = DZ; % pre-allocate
DY = cell(1,ntransects); DY2 = DY; % pre-allocate

for j6=1:ntransects

    % First derivatives
    % DZ{j6} will have one less element than zp_subaerial{j6}
    % DY{j6} will have one less element than yp_subaerial{j6}
    DZ{j6}= diff(zp_subaerial{j6});
    DY{j6}= diff(yp_subaerial{j6});

    % Second derivatives
    % DZ2{j6} will have 2 less elements than zp_subaerial{j6}
    % DY2{j6} will have 2 less elements than yp_subaerial{j6}
    DZ2{1,j6}= (diff(zp_subaerial{1,j6},2));
    DY2{1,j6}= (diff(yp_subaerial{1,j6},2));
end
```

```
%% Indexing
% find steepest part of slope for each transect
steepestIndex = cell(1,ntransects);
steepestY = cell(1,ntransects);
bufferDist = cell(1,ntransects);
bufferIndex = cell(1,ntransects);
crestIndex = cell(1,ntransects);
yCrest = cell(1,ntransects);
toeIndex = cell(1,ntransects);
yToe = cell(1,ntransects);
slopeScarp = cell(1,ntransects);
ScarpHeight = cell(1,ntransects);
seawardIndex = cell(1,ntransects);
yseaward = cell(1,ntransects);
foreshoreslope =  cell(1,ntransects);

for j7=1:ntransects
   steepestIndex{j7} = find(DZ{j7}==min(DZ{j7})); % index of steepest section in profile
   steepestY{j7} = yp_subaerial{j7}(steepestIndex{j7}); % y-coord of steepest part

   bufferDist{j7} = steepestY{j7}+slopeBuffer; % toe buffer

   if length(bufferDist{j7})>1 % take first point (nearest to shore)
      bufferDist{j7} = bufferDist{j7}(1,1);
   end

   % Find index of most seaward point before the toe buffer point in yp_subaerial
   bufferIndex{j7} = find(yp_subaerial{j7} < bufferDist{j7}, 1, 'last');


   % Limit the bufferindex to the length of the second derivative
   % this only matters if it doesn't find a scarp
   bufferIndex{j7} = min(bufferIndex{j7},length(DZ2{1,j7}));


   crestIndex{j7} =  find(DZ2{j7} == min(DZ2{j7}(1:bufferIndex{j7})), 1, 'first');
   yCrest{j7} = yp_subaerial{j7}(crestIndex{j7})+1;

   toeIndex{j7} =  find(DZ2{j7} == max(DZ2{j7}(crestIndex{j7}:bufferIndex{j7})), 1, 'first');
   yToe{j7} = yp_subaerial{j7}(toeIndex{j7})+1;

   seawardIndex{j7} = find(zvals{j7} <=  (-1),1,'last');
   yseaward{j7} = yvals(seawardIndex{j7});

   if toeIndex{j7}-crestIndex{j7} > 35;
      crestIndex{j7}= find(DZ2{j7} == min(DZ2{j7}((crestIndex{j7}+2):toeIndex{j7})), 1, 'first');
      yCrest{j7}=  yp_subaerial{j7}(crestIndex{j7})+1
   end
```

```
% Calculate slope and height in buffer zone (where scarp is suspected) & foreshore slope from
toe to -2.5 m NAP
    foreshoreslope{j7} = ((zp_subaerial{j7}(toeIndex{j7})-zvals{j7}(seawardIndex{j7}))/(yToe{j7}-
        yseaward{j7}));
   slopeScarp{j7} = ((zp_subaerial{j7}(toeIndex{j7})-zp_subaerial{j7}(crestIndex{j7}))/(yToe{j7}-
        yCrest{j7}));
   ScarpHeight{j7} = (zp_subaerial{j7}(toeIndex{j7})-zp_subaerial{j7}(crestIndex{j7}));

   if (ScarpHeight {j7} >= -0.30) || (slopeScarp {j7} >= -0.15)
      yCrest{j7} = NaN;
      crestIndex{j7} = NaN;
      yToe{j7} = NaN;
      toeIndex{j7} = NaN;
      ScarpHeight{j7} = NaN;
      slopeScarp{j7} = NaN;
      foreshoreslope{j7} = NaN;
  end
end
```

Appendix F - Study Site Photos

All pictures were taken by John Darnall and Stuart Pearson on February 3rd, 2016

Beach scarps at the Sand Engine in the order of ~ 10 cm. The **notching** as a result of undercutting can be clearly seen in both figures #1 & #2.

Beach scarp in the order of ~ 1 m. The stratigraphy in the scarp face is pronounced. Also, it appears aeolian transport has had some erosional effect insinuating this scarp has been in existence for a substantial amount of time.

Small scarp (~ 15 cm) at the point of the Sand Engine. The overhanging sediment is still in tact, but the sand still appears wet. As this sand dries, notching may occur similar to figure #1 & #2.

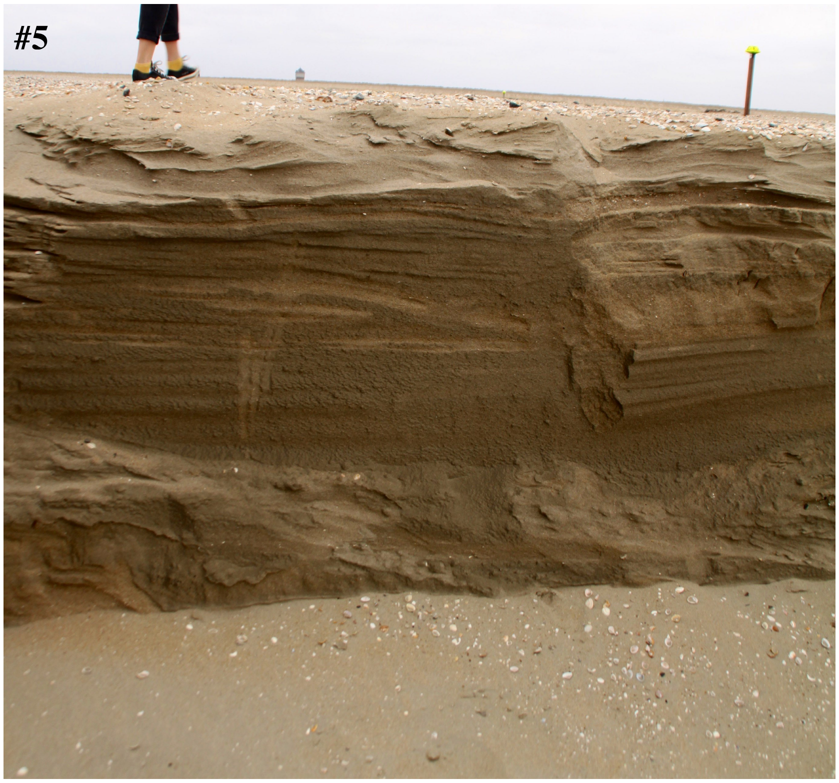

~ 1 m scarp at the head of the Sand Engine. The stratigraphy in sand layers is very pronounced and similar to the stratigraphy at the mouth of the lagoon (see figure #6). This also demonstrates the safety concerns of these features quite nicely.

Scarp-like features along the sandbanks near the mouth of the lagoon. The tidal currents through this region are very strong, which is an indicator that longshore currents play a significant role in beach scarping.

Beach scarp in the order of ~ 1 m at the Sand Engine (#7), and the pronounced runnel and sand bar just seaward of this feature (#8).

Beach scarp in the order of ~ 1 m. The stratigraphy in the scarp face is pronounced. Also,the shell patterns and 'tough' material show interesting patterns in the scarp face.

Remnants of a beach scarp. It appears the adjacent segments were washed away, but this small section still remained.

#11

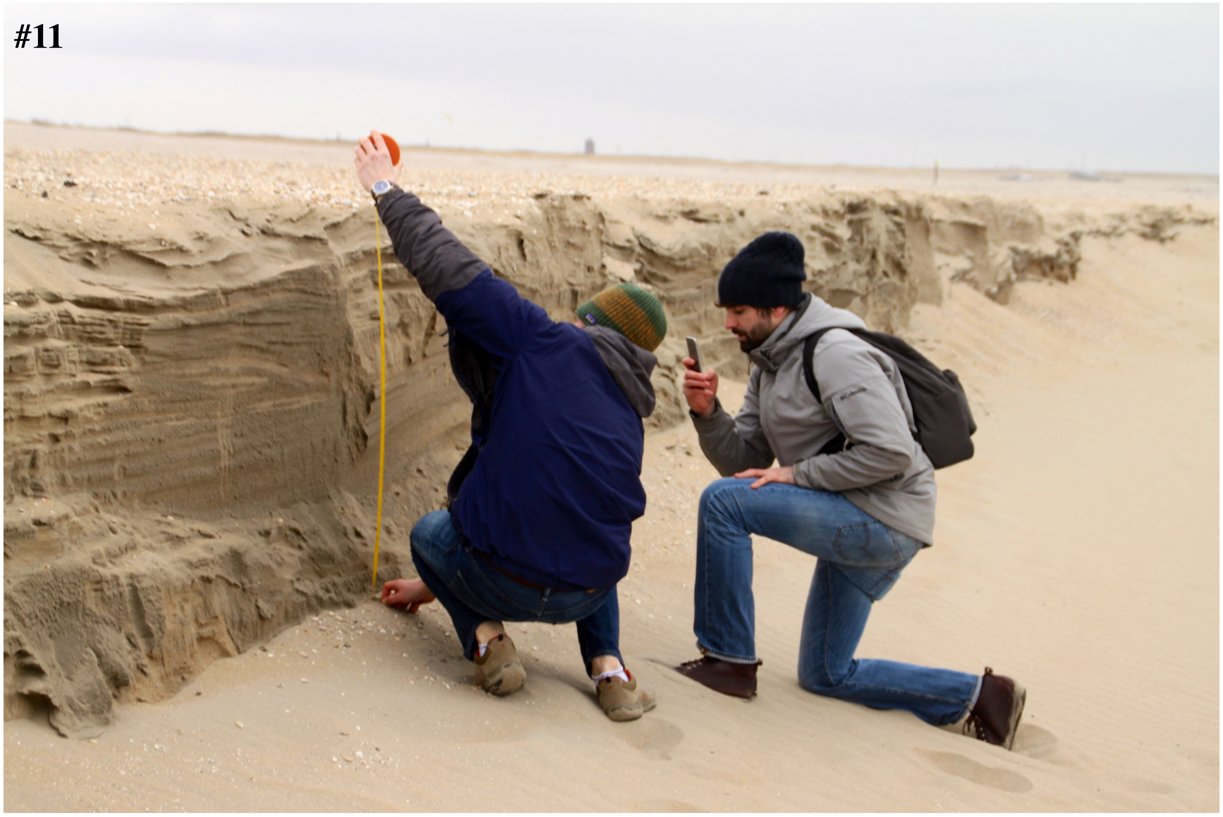

90 cm beach scarp with longshore height variability. Aeolian transport appears to have influenced this scarp insinuating it has existed for a significant amount of time.